

The C3-OH of Amphotericin B Plays an Important Role in Ion Conductance

Stephen A. Davis,² Lisa A. Della Ripa,² Lingbowei Hu,³ Alexander G. Cioffi,³ Taras V. Pogorelov,^{4,5} Chad M. Rienstra,^{2,*} and Martin D. Burke^{1,2,*}

¹Howard Hughes Medical Institute, ²Roger Adam Laboratory, Department of Chemistry, ³Department of Biochemistry, ⁴School of Chemical Sciences, ⁵National Center for Supercomputing Applications, University of Illinois at Urbana-Champaign, Urbana, IL 61801, United States

Supporting Information

Part A

- I. General Methods
- II. Synthesis of AmB Derivatives
- III. Planar Lipid Bilayer Experiments
- IV. Liposome Efflux Experiments

Part B

- I. NMR Studies
- II. Computational Conformational Search with Energy Minimization Calculations
- III. NMR Spectra of New Compounds

Part A

I. General Methods

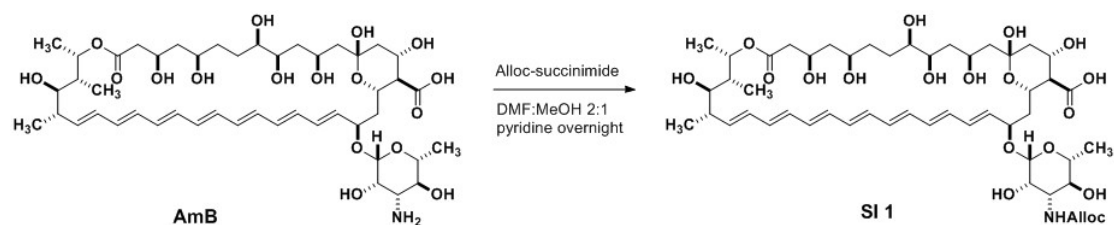
Materials. Commercially available materials were purchased from Sigma-Aldrich Co. (Milwaukee, WI), Fisher Scientific (Hampton, NH), AK Scientific (Union City, CA) and used without further purifications unless noted otherwise. Camphorsulfonic acid was recrystallized from the ethyl acetate prior to use. All solvents were dispensed from a solvent purification system that passes solvents through packed columns according to the method of Pangborn and coworkers¹ (THF, CH₂Cl₂, toluene, hexanes: dry neutral alumina; DMSO, DMF, CH₃OH: activated molecular sieves). Triethylamine, *N,N*-diisopropylethylamine and pyridine were freshly distilled under nitrogen from CaH₂. Water was double distilled or obtained from a Millipore MilliQ water purification system.

Reactions. Due to the light and air sensitivity of Amphotericin B, all manipulations were carried out under low light conditions and compounds were stored under an anaerobic atmosphere. All

reactions were performed in oven- or flame-dried glassware under an atmosphere of argon unless otherwise indicated. Reactions were monitored by analytical thin layer chromatography performed using the indicated solvent on E. Merck silica gel 60 F₂₅₄ plates (0.25 mm). Compounds were visualized using a UV (λ_{254}) lamp or stained by KMnO₄. Alternatively, reactions were monitored by RP-HPLC using an Agilent 1100 series HPLC system equipped with a Symmetry[®]C₁₈ 5 micron 4.6 x 150 mm column (Waters Corp. Milford, MA) with UV detection at 383 nm and the indicated eluent and flow rate of 1.2 mL/min.

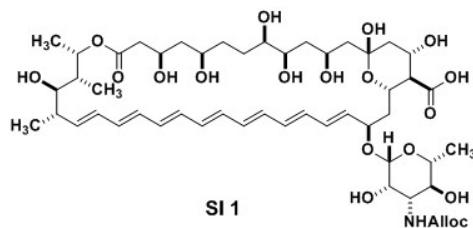
Purification and Analysis. Flash chromatography was performed as described by Still and coworkers² using the indicated solvent on E. Merck silica gel 60 230-400 mesh. ¹H NMR spectra were recorded at 23 °C on one of the following instruments: Varian Unity 500, Varian VXR 500, Agilent VNS 750. Chemical shifts (δ) are reported in parts per million (ppm) downfield from tetramethylsilane and referenced internally to the residual protium in the NMR solvent (CD₃C(O)CHD₂, δ = 2.04, center line) or to added tetramethylsilane. Data are reported as follows: chemical shift, multiplicity (s = singlet, d = doublet, t = triplet, q = quartet, p = pentet, dd = doublet of doublets, app. = apparent), coupling constant (*J*) in Hertz (Hz) and integration. ¹³C spectra were recorded at 23 °C with Varian Unity 500 or Varian VXR 500. Chemical shift (δ) are reported downfield of tetramethylsilane and are referenced to the carbon resonances in the NMR solvent (CD₃C(O)CD₃, δ = 39.5, center line) or to added tetramethylsilane. High resolution mass spectra (HRMS) were obtained at the University of Illinois mass spectrometry facility. All synthesized compounds gave HRMS within 5 ppm of calculated values.

II. Synthesis of AmB derivatives



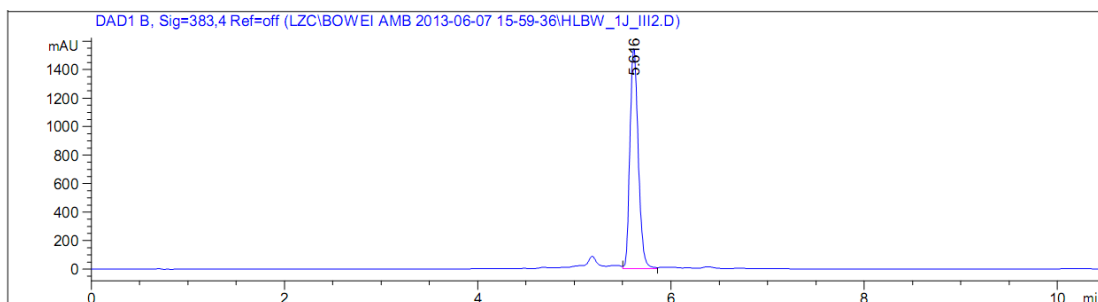
N-Alloc SI 1

A round bottom flask was charged with Amphotericin B (4 g, 4.33 mmol, 1 eq) which were dissolved in a mixture of DMF: MeOH 2:1 (135 mL) at 23 °C. Pyridine (4 mL, 49.4 mmol, 11.4 eq), Alloc-succinimide (2.4 g, 12.1 mmol, 2.8 eq) was subsequently added and the reaction was stirred overnight. The reaction mixture was then poured into diethyl ether (4 L). After stirring for 15 minutes, the resulting yellow precipitate was isolated via Buchner filtration using Whatman 50 filter paper and washed with diethyl ether to afford a yellow solid (4.32 g, 4.28 mmol, 99 %). This material was carried forward without further purification.



HPLC (C₁₈ SiO₂; flow rate = 1.2 mL/min; MeCN: 25 mM NH₄OAc in H₂O 1:19 → 19:1 over 8 minutes)

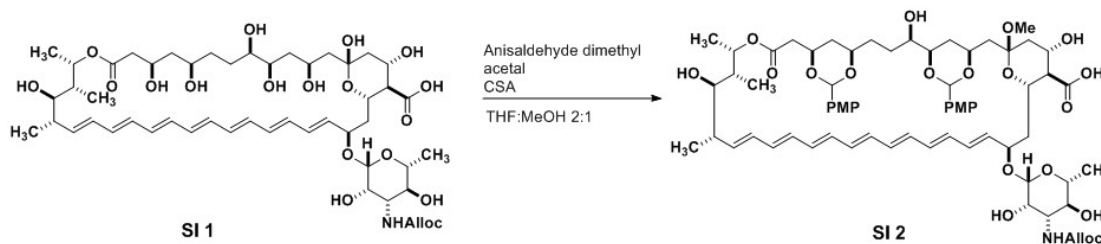
tR: 5.6 min



HRMS (ESI)

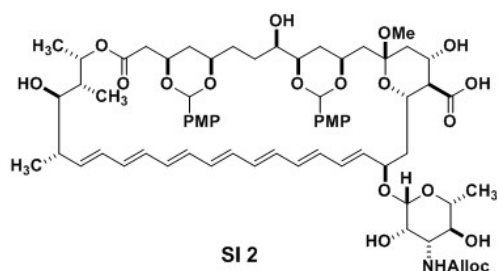
Calculated for C₅₁H₇₇NO₁₉(M+Na)⁺: 1030.4987

Found: 1030.4968



***p*-methoxybenzylideneacetal methyl ketal SI 2**

A round bottom flask was charged with **SI 1** (6 g, 5.95 mmol, 1 eq) which was dissolved in a mixture of THF: MeOH 2:1 (198 mL) at 23 °C. Camphorsulfonic acid (350 mg, 1.51 mmol, 0.25 eq) was added followed by anisaldehyde dimethyl acetal (10 mL, 58.7 mmol, 9.9 eq). The resulting mixture was quenched with triethylamine (240 μL, 2.96 mmol, 0.5 eq) after 45 minutes at 23 °C. The mixture was then concentrated in vacuo to form brown oil. Purification of the crude oil by flash chromatography (SiO₂; methylene chloride: methanol 97:3 → 93:7, 0.1 % AcOH) furnished **SI 2** as an orange solid (4.15 g, 3.30 mmol, 56 %).



TLC (methylene chloride: MeOH 9:1, 0.1 %AcOH)

$R_f = 0.44$, visualized by UV

$^1\text{H NMR}$ (500 MHz, acetone *d*-6)

δ 7.44 (d, $J = 8.5$ Hz, 2H), 7.36 (d, $J = 8.8$ Hz, 2H), 6.92-6.85 (m, 4H), 6.50-6.17 (m, 11H), 6.03 (app d, $J = 8.8$ Hz, 1H), 5.99-5.87 (m, 2H), 5.58 (dd, $J = 9.4$ Hz, $J = 14.1$ Hz, 1H), 5.53 (s, 1H), 5.46 (s, 1H), 5.31 (dd, $J = 1.3$ Hz, $J = 17.5$ Hz, 1H), 5.30-5.23 (m, 1H), 5.19-5.13 (m, 1H), 4.70 (app t, $J = 5.6$ Hz, 1H), 4.64 (s, 1H), 4.58-4.48 (m, 2H), 4.23-4.13 (m, 2H), 3.99-3.91 (m, 2H), 3.85-3.70 (m, 8H), 3.62-3.56 (m, 2H), 3.48-3.41 (m, 2H), 3.40-3.28 (m, 3H), 3.07 (s, 3H), 2.58 (dd, $J = 6.0$ Hz, $J = 6.0$ Hz, 1H), 2.46-2.38 (m, 1H), 2.37-2.29 (m, 2H), 2.27-2.20 (m, 1H), 2.15-2.10 (m, 1H), 1.94-1.81 (m, 3H), 1.78-1.60 (m, 3H), 1.60-1.43 (m, 4H), 1.39-1.32 (m, 2H), 1.24 (d, $J = 5.5$ Hz, 3H), 1.23-1.22 (m, 1H), 1.19 (d, $J = 6.6$ Hz, 3H), 1.11 (d, $J = 6.6$ Hz, 3H), 1.02 (d, $J = 7.1$ Hz, 3H)

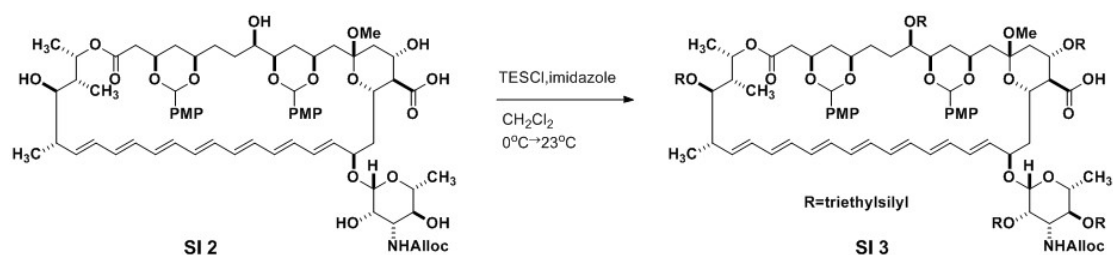
$^{13}\text{C NMR}$ (125 MHz, acetone *d*-6)

δ 172.1, 169.8, 160.7, 160.6, 157.5, 137.7, 136.4, 134.6, 134.4, 134.2 (2C), 134.1, 134.0, 133.9, 133.7, 133.1, 132.8, 132.7, 132.4, 130.0, 128.4 (2C), 117.3, 114.3, 114.0, 101.2, 100.9, 100.8, 98.2, 95.0, 81.2, 78.2, 76.4, 74.8, 74.3, 73.4, 73.3, 73.1, 72.5, 72.3, 71.8, 71.1, 70.7, 69.3, 67.4, 67.2, 65.8, 65.7, 57.9, 57.2, 55.6, 54.9, 48.7, 43.7, 42.8, 41.9, 41.7, 38.1, 37.0, 34.1, 33.3, 28.9, 20.5, 18.8, 18.4 (2C), 17.6, 12.0

HRMS (ESI)

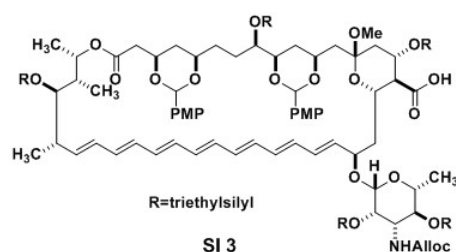
Calculated for $\text{C}_{67}\text{H}_{91}\text{NO}_{21}$ ($\text{M}+\text{Na}$) $^+$: 1280.5981

Found: 1280.5939



Pentatriethylsilyl ether **SI 3**

SI 2 (4 g, 3.18 mmol, 1 eq) and imidazole (4.3 g, 63.6 mmol, 20 eq) were added into a round bottom flask which were then azeotropically dried via co-evaporation with toluene. The resulting solid was dissolved in methylene chloride (106 mL) and cooled to 0 °C. Triethylsilyl chloride (5.3 mL, 31.8 mmol, 10 eq) was added dropwise over 3 minutes. The resulting yellow suspension was warmed to 23 °C and stirred for 4 hours. The mixture was then quenched at 0 °C with saturated aqueous sodium bicarbonate (106 mL), which was then diluted with diethyl ether (1 L) and the layers were separated. The organic layer was washed with water: saturated aqueous sodium bicarbonate 1:1 (3 x 250 mL) and brine (1 x 250 mL), dried over sodium sulfate and concentrated in vacuo. Purification of the crude brown oil by flash chromatography (SiO₂; hexanes: ethyl acetate 19:1→ 4:1, 0.1 % AcOH) furnished **SI 3** as an orange solid (1.92 g, 1.87 mmol, 59 %).



TLC (hexane:ethyl acetate 7:3, 0.1 % AcOH)

$R_f=0.71$, visualized by UV

¹H NMR (500 MHz, acetone *d*-6)

δ 7.44-7.34 (m, 4H), 6.93-6.85 (m, 4H), 6.49-6.05 (m, 12H), 6.00-5.91 (m, 1H), 5.87 (app dd, $J = 5.6$ Hz, $J = 14.7$ Hz, 1H), 5.66 (dd, $J = 9.3$ Hz, $J = 15.1$ Hz, 1H), 5.46 (app s, 2H), 5.42-5.38 (m, 1H), 5.37-5.30 (m, 1H), 5.22-5.15 (m, 1H), 4.99-4.90 (m, 1H), 4.72-4.67 (m, 1H), 4.62-4.49 (m, 3H), 4.27 (dt, $J = 4.5$ Hz, $J = 10.5$ Hz, 1H), 4.23-4.14 (m, 1H), 3.97-3.87 (m, 3H), 3.79 (s, 3H), 3.81-3.67 (m, 7H), 3.63-3.56 (m, 1H), 3.48 (app t, $J = 9.0$ Hz, 1H), 3.36-3.28 (m, 1H), 3.08 (s, 3H), 2.54 (dd, $J = 7.4$ Hz, $J = 17.5$ Hz, 1H), 2.45-2.37 (m, 1H), 2.33-2.23 (m, 3H), 2.13-2.07 (m, 1H), 1.96-1.84 (m, 3H), 1.79-1.53 (m, 4H), 1.53-1.41 (m, 4H), 1.36-1.26 (m, 1H), 1.25 (d, $J = 6.1$ Hz, 3H), 1.23-1.20 (m, 1H), 1.19 (d, $J = 6.1$ Hz, 3H), 1.09-0.76 (m, 49H), 0.76-0.40 (m, 32H)

¹³C NMR (125 MHz, acetone *d*-6)

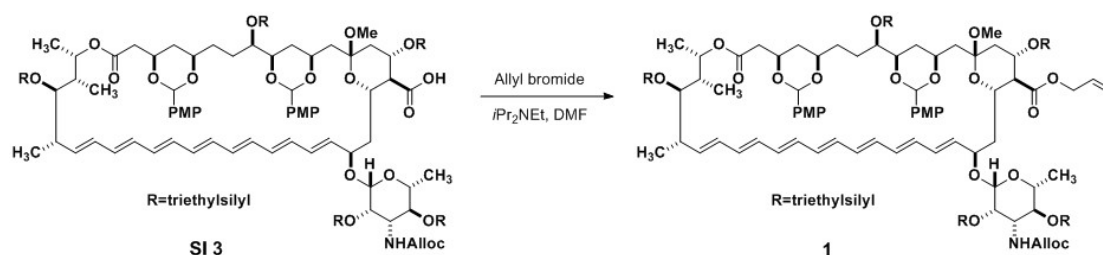
δ 174.1, 170.0, 160.9, 160.8, 156.4, 136.5, 134.7, 134.6, 134.5, 134.4, 134.2, 133.7, 133.6, 133.4, 133.1, 132.9, 132.8, 132.7, 131.5, 131.2, 128.7, 128.4, 117.4, 114.3, 114.0, 113.9, 101.8, 101.2, 101.0, 98.3, 81.7, 76.3, 75.3, 75.2, 74.6, 74.0, 73.4, 73.2, 73.0, 71.9, 68.8, 67.8, 65.9, 58.3, 57.2, 55.6, 48.5, 44.1, 43.4, 41.4, 41.2, 38.0, 36.6, 33.7, 33.0, 28.4, 19.0, 18.6, 18.3, 7.5, 7.3 (2C), 7.2, 7.1, 7.0, 6.7, 6.2, 6.0 (2C), 5.9 (2C), 5.8, 5.7, 5.6

HRMS (ESI)

Calculated for C₉₈H₁₆₁NO₂₁Si₅ (M+Na)⁺: 1851.0305

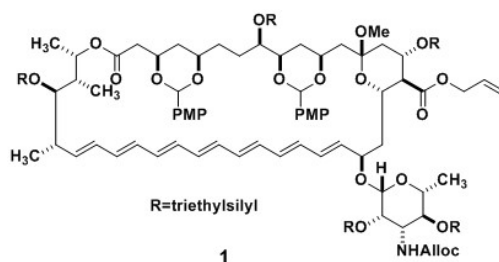
Found :

1851.0310



Allyl ester 1

To a stirred solution of **SI 3** (1.62 g, 0.885 mmol, 1 eq) in dimethylformamide (29.5 mL) was added allyl bromide (3.1 mL, 35.4 mmol, 40 eq) and *N,N*-diisopropylethylamine (0.62 mL, 3.54 mmol, 4 eq). The solution was stirred for 4 hours at 23 °C and then diluted with diethyl ether (300 mL). The resulting mixture was washed with water: saturated aqueous ammonium chloride 1:1 (3 x 75 mL) and brine (1 x 75 mL). The organic layer was dried over sodium sulfate and then concentrated in vacuo. Purification by flash chromatography (SiO₂; hexanes: ethyl acetate 19:1 → 9:1) afforded **1** as an orange solid (1.42 g, 0.763 mmol, 86 %).



TLC (hexanes: ethyl acetate 7:3)

$R_f = 0.78$, visualized by UV

¹H NMR (500 MHz, acetone *d*-6)

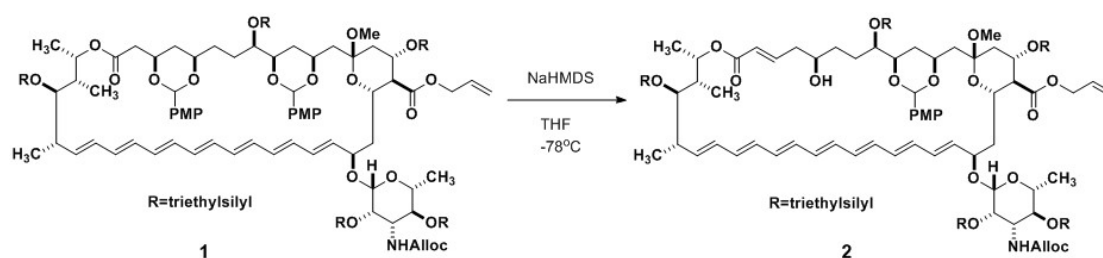
δ 7.44-7.35 (m, 4H), 6.93-6.85 (m, 4H), 6.52-6.17 (m, 11H), 6.12 (dd, $J = 9.8$ Hz, $J = 15.0$ Hz, 1H), 6.05-5.90 (m, 2H), 5.90-5.83 (m, 1H), 5.66 (dd, $J = 9.2$ Hz, $J = 14.9$ Hz, 1H), 5.54-5.26 (m, 6H), 5.23-5.16 (m, 1H), 5.00-4.92 (m, 1H), 4.76-4.51 (m, 5H), 4.50 (s, 1H), 4.28 (dt, $J = 4.6$ Hz, $J = 10.6$ Hz, 1H), 4.25-4.16 (m, 1H), 3.97-3.87 (m, 3H), 3.79 (s, 3H), 3.78 (s, 3H), 3.77-3.67 (m, 4H), 3.65 (app dt, $J = 3.2$ Hz, $J = 9.6$ Hz, 1H), 3.48 (t, $J = 8.9$ Hz, 1H), 3.38-3.29 (m, 1H), 3.08 (s, 3H), 2.54 (dd, $J = 7.3$ Hz, $J = 17.5$ Hz, 1H), 2.46-2.39 (m, 1H), 2.36-2.25 (m, 3H), 2.04-1.98 (m, 1H), 1.97-1.84 (m, 3H), 1.80-1.53 (m, 6H), 1.53-1.40 (m, 2H), 1.37-1.28 (m, 2H), 1.24 (d, $J = 6.2$ Hz, 3H), 1.19 (d, $J = 6.2$ Hz, 3H), 1.08-0.86 (m, 49H), 0.76-0.37 (m, 32H)

¹³C NMR (125 MHz, acetone *d*-6)

δ 172.7, 169.7, 160.6, 160.5, 156.1, 136.4, 134.6, 134.5, 134.3, 134.2, 134.1, 133.6, 133.5 (2C), 133.3, 133.1, 132.7, 132.5, 132.4, 131.4, 131.0, 128.5, 128.2, 128.0 (2C), 127.9, 118.9, 117.3, 114.1, 113.8, 113.7, 101.7, 101.0, 100.7, 98.7, 81.5, 75.9, 75.7, 74.9, 74.5, 73.7, 73.0, 72.7, 71.6, 68.7, 67.5, 65.7 (2C), 58.1, 57.7, 55.5, 55.4 (2C), 48.4, 43.8, 43.1, 41.3, 37.8, 36.6, 33.4, 32.7, 28.0, 19.0, 18.5, 18.4, 11.3, 7.6, 7.4 (2C), 7.3 (2C), 7.2, 7.1, 6.2, 6.1 (2C), 6.0, 5.9 (2C), 5.8, 5.7, 5.6 (3C), 5.5, 5.2

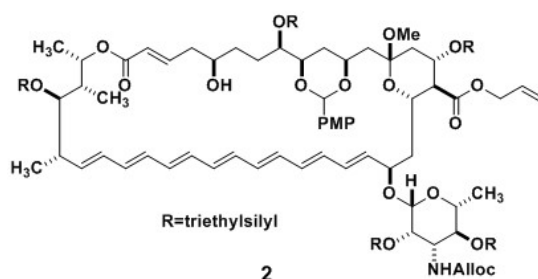
HRMS (ESI)

Calculated for $C_{101}H_{165}NO_{21}Si_5$ ($M+Na$)⁺: 1891.0618
 Found: 1891.0547



α,β -unsaturated lactone **2**

Prior to the reaction, **1** (1.63 g, 0.872 mmol, 1 eq) was azeotropically dried via coevaporation with toluene. The resulting orange solid was dissolved in THF (14.5 mL) and cooled to -78°C . Sodium bis(trimethylsilyl)amide (800 mg, 4.36 mmol, 5 eq) in THF (14.5 mL) was cooled to -78°C and added dropwise into the solution of **1** over 5 minutes via syringe. The mixture was stirred for 1 hour at -78°C and quenched with saturated aqueous ammonium chloride (29 mL) at -78°C , which was then extracted with diethyl ether (300 mL). The organic layer was washed with water: saturated aqueous ammonium chloride 1:1 (3 x 75 mL) and brine (1 x 75 mL), dried over sodium sulfate, and concentrated in vacuo. Purification of the crude orange oil by flash chromatography (SiO_2 ; hexanes: ethyl acetate 19:1 \rightarrow 17:3) afforded **2** as a yellow solid (1.14 g, 0.658 mmol, 75 %).



TLC (hexanes: ethyl acetate 7:3)

$R_f=0.74$, visualized by UV

¹H NMR (500 MHz, acetone *d*-6)

δ 7.40 (app d, *J* = 6.7 Hz, 2H), 6.97 (dt, *J* = 15.6 Hz, *J* = 7.0 Hz, 1H), 6.90 (app d, *J* = 6.7 Hz, 2H), 6.47-6.07 (m, 12H), 6.04-5.85 (m, 3H), 5.80 (d, *J* = 15.6 Hz, 1H), 5.62 (dd, *J* = 8.9 Hz, *J* = 14.0 Hz, 1H), 5.47 (s, 1H), 5.46-5.25 (m, 4H), 5.19 (dq, *J* = 10.5 Hz, *J* = 4.6 Hz, 1H), 5.12-5.05 (m, 1H), 4.69 (dd, *J* = 6.0 Hz, *J* = 13.6 Hz, 1H), 4.66-4.53 (m, 4H), 4.52 (s, 1H), 4.28 (dt, *J* = 4.7 Hz, *J* = 10.6 Hz, 1H), 3.99-3.89 (m, 3H), 3.81-3.73 (m, 4H), 3.72-3.67 (m, 2H), 3.68-3.60 (m, 2H), 3.48 (t, *J* = 8.9 Hz, 1H), 3.34-3.27 (m, 1H), 3.13 (s, 3H), 2.49-2.25 (m, 6H), 2.03-1.89 (m, 4H), 1.88-1.80 (m, 1H), 1.73-1.43 (m, 5H), 1.40-1.32 (m, 1H), 1.22 (d, *J* = 6.2 Hz, 3H), 1.20 (d, *J* = 6.1 Hz, 3H), 1.07 (d, *J* = 6.8 Hz, 3H), 1.05-0.77 (m, 46H), 0.75-0.38 (m, 32H)

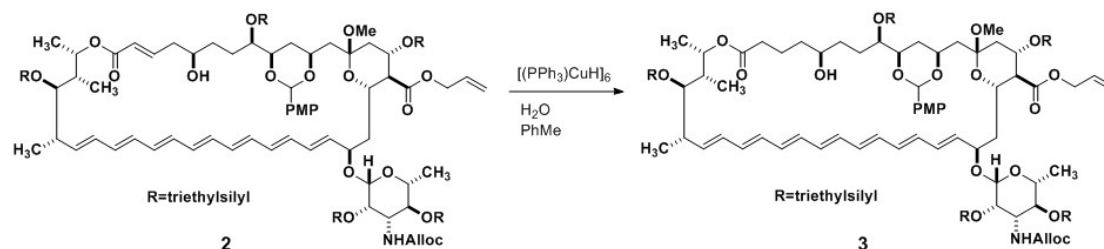
¹³C NMR (125 MHz, acetone *d*-6)

δ 172.6, 165.7, 160.6, 156.0, 147.3, 137.7, 136.5, 134.2, 134.1, 134.0, 133.9, 133.7 (2C), 133.5, 133.3, 133.2, 132.8, 132.6, 132.4, 131.8, 130.4, 128.5, 123.5, 118.9, 117.2, 113.7, 101.6, 100.8, 98.7, 81.4, 78.9, 75.9, 75.1, 74.4, 73.7, 73.2, 73.0, 70.7, 70.3, 68.6, 67.5, 65.7, 65.6, 58.1, 57.1, 55.4, 48.5, 43.8, 42.9, 41.9, 37.2, 34.3, 33.2, 28.9, 18.9, 18.6, 18.1, 12.2, 7.4 (2C), 7.3, 7.2, 7.0, 5.8, 5.7 (2C), 5.4

HRMS (ESI)

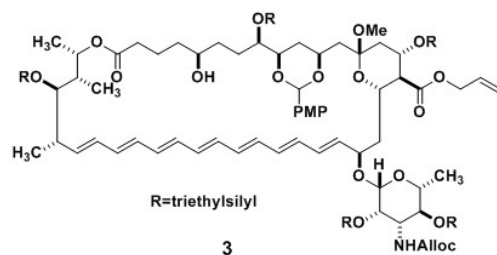
Calculated for C₉₃H₁₅₇NO₁₉Si₅ (M+Na)⁺: 1755.0094

Found: 1755.0094



Lactone **3**

A round bottom flask was purged with argon and charged with **2** (500 mg, 0.288 mmol, 1 eq) and Stryker's reagent (566 mg, 0.288 mmol, 1 eq). Toluene (14.4 mL) and water (45 μL) was subsequently added and the mixture was stirred for 14 hours at 23 °C. The mixture was then stirred under air for 30 minutes before it was filtered through celite plug with ethyl acetate (600 mL). The filtrate was washed with water: saturated aqueous ammonium chloride 1:1 (2 x 150 mL), water: saturated aqueous sodium bicarbonate 1:1 (2 x 150 mL) and brine (1 x 150 mL). The organic layer was dried over sodium sulfate and concentrated in vacuo. Purification by flash chromatography (SiO₂; hexanes: ethyl acetate 19:1 → 17:3) afforded **3** as a yellow solid (424 mg, 0.244 mmol, 85 %).



TLC (hexanes: ethyl acetate 7:3)

$R_f=0.68$, visualized by UV

^1H NMR (500 MHz, acetone *d*-6)

δ 7.40 (d, $J=8.7$ Hz, 2H), 6.90 (d, $J=8.7$ Hz, 2H), 6.46-6.08 (m, 12H), 6.05-5.92 (m, 2H), 5.89 (m, 1H), 5.61 (dd, $J=9.2$ Hz, $J=14.5$ Hz, 1H), 5.47 (s, 1H), 5.46-5.26 (m, 4H), 5.19 (app dd, $J=1.5$ Hz, $J=10.5$ Hz, 1H), 4.98 (m, 1H), 4.69 (dd, $J=5.8$ Hz, $J=13.4$ Hz, 1H), 4.66-4.52 (m, 4H), 4.50 (s, 1H), 4.28 (dt, $J=4.6$ Hz, $J=10.7$ Hz, 1H), 3.98-3.88 (m, 3H), 3.79 (s, 3H), 3.77-3.67 (m, 4H), 3.64 (m, 1H), 3.48 (t, $J=8.9$ Hz, 1H), 3.31 (m, 1H), 3.11 (s, 3H), 2.42 (m, 1H), 2.34-2.18 (m, 4H), 2.15 (m, 1H), 2.12 (m, 1H), 2.01 (m, 1H), 1.95 (m, 1H), 1.90-1.82 (m, 4H), 1.80-1.58 (m, 5H), 1.55-1.48 (m, 3H), 1.24 (d, $J=6.0$ Hz, 3H), 1.18 (d, $J=6.2$ Hz, 3H), 1.06 (d, $J=6.7$ Hz, 3H), 1.04-0.78 (m, 46H), 0.76-0.36 (m, 32H)

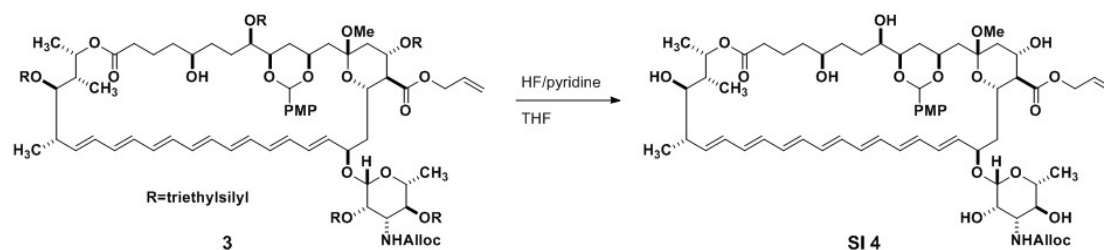
^{13}C NMR (125 MHz, acetone *d*-6)

δ 172.9, 172.7, 160.9, 156.3, 138.5, 136.7, 134.5, 134.2, 134.1, 134.0, 133.8, 133.7, 133.6, 133.5 (2C), 132.9, 132.8, 132.7, 132.6, 131.5, 130.5, 129.5, 129.4, 128.7, 126.1, 119.0, 117.3, 113.9, 110.6, 101.9, 101.0, 98.9, 81.8, 78.4, 76.0, 75.3, 74.7, 73.9, 73.4, 73.3, 71.2, 71.1, 68.8, 67.8, 65.9, 65.8, 58.4, 57.4, 55.6, 48.6, 44.1, 43.2, 41.3, 39.2, 37.4, 35.2, 34.5, 33.4, 29.1, 21.7, 19.0, 18.6, 18.4, 11.8, 7.4 (2C), 7.3, 7.1, 6.0 (2C), 5.9(2C), 5.6

HRMS (ESI)

Calculated for $\text{C}_{93}\text{H}_{159}\text{NO}_{19}\text{Si}_5$ ($\text{M}+\text{Na}$) $^+$: 1757.0250

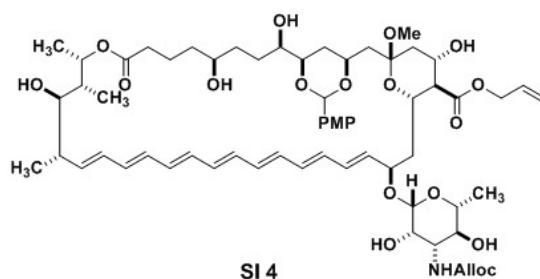
Found: 1757.0303



Polyol SI 4

A plastic bottle was charged with **3** (1 g, 0.576 mmol, 1 eq), which was dissolved in THF (20 mL)

and cooled to 0 °C. A pyridine (36.8 mL) and THF (60 mL) mixture in another plastic bottle was cooled to 0 °C. 70 % HF-pyridine was added to another plastic bottle containing pyridine (36.8 mL) and THF (60 mL) at 0°C. The resulting solution was then cannula transferred slowly to the THF solution of **3** and the reaction was allowed to stir at 23 °C. After 12 hours the reaction was quenched at 0 °C with saturated aqueous sodium bicarbonate and diluted with methylene chloride (1.2 L). The organic layer was washed with water: saturated aqueous sodium bicarbonate 1:1 (2 x 600 mL) and brine (600 mL). The organic layer was dried with sodium sulfate and concentrated in vacuo. Purification by flash chromatography (SiO₂; methylene chloride: MeOH 99:1 → 95:5) afforded **SI 4** as a yellow solid (587.2 mg, 0.504 mmol, 88 %).



TLC (methylene chloride: MeOH 9:1)

R_f = 0.46, visualized by UV

¹H NMR (500 MHz, acetone *d*-6)

δ 7.45 (d, J = 8.7 Hz, 2H), 6.89 (d, J = 8.6 Hz, 2H), 6.47-6.29 (m, 9H), 6.27-6.17 (m, 3H), 6.08 (app d, J = 8.8 Hz, 1H), 6.03-5.90 (m, 3H), 5.59 (dd, J = 9.1 Hz, J = 14.3 Hz, 1H), 5.54 (s, 1H), 5.43 (app dd, J = 1.6 Hz, J = 17.2 Hz, 1H), 5.32 (app dd, J = 1.4 Hz, J = 17.2 Hz, 1H), 5.26 (app dd, J = 1.4 Hz, J = 10.6 Hz, 1H), 5.22-5.14 (m, 2H), 5.16 (dq, J = 10.6 Hz, J = 1.5 Hz, 1H), 4.72-4.62 (m, 3H), 4.59 (s, 1H), 4.56-4.49 (m, 2H), 4.19 (dt, J = 4.8 Hz, J = 10.1 Hz, 1H), 4.01-3.90 (m, 2H), 3.84 (app d, J = 2.0 Hz, 1H), 3.79 (s, 3H), 3.77-3.72 (m, 1H), 3.67-3.59 (m, 1H), 3.48-3.28 (m, 5H), 3.11 (s, 3H), 2.48-2.34 (m, 2H), 2.31 (app t, J = 10.1 Hz, 1H), 2.26-2.18 (m, 2H), 2.18-2.11 (m, 2H), 2.04-1.99 (m, 1H), 1.92-1.83 (m, 3H), 1.80-1.71 (m, 2H), 1.66-1.58 (m, 1H), 1.57-1.45 (m, 3H), 1.43-1.31 (m, 3H), 1.26 (d, J = 5.2 Hz, 3H), 1.20 (d, J = 6.0 Hz, 3H), 1.13 (d, J = 6.4 Hz, 3H), 1.02 (d, J = 7.2 Hz, 3H)

¹³C NMR (125 MHz, acetone *d*-6)

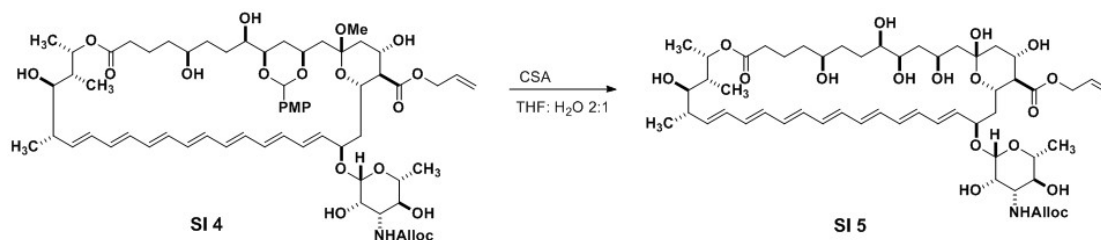
δ 172.9, 172.7, 160.6, 157.3, 137.7, 136.8, 134.6, 134.5, 134.1, 134.0, 133.9 (2C), 133.8 (2C), 133.6 (2C), 132.8, 132.7, 132.5, 132.2, 129.5, 128.4, 118.5, 117.1, 113.9, 101.0, 100.8, 98.3, 81.2, 78.3, 74.9, 74.3, 74.2, 73.1, 72.1, 71.9, 71.2, 70.2, 67.3, 67.2, 65.7, 65.6 (2C), 58.0, 57.5, 55.5, 48.9, 43.6, 43.5, 42.6, 41.6, 39.1, 37.4, 35.7, 35.3, 33.9, 30.6, 27.2, 22.1, 18.8, 18.4, 17.6, 12.2

HRMS (ESI)

Calculated for C₆₃H₈₉NO₁₉ (M+Na)⁺: 1186.5926

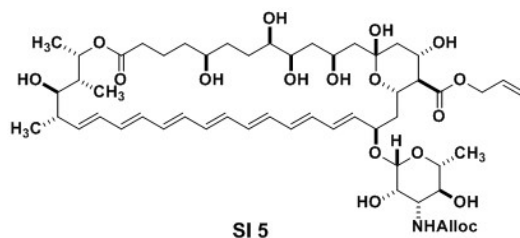
Found:

1186.5951



Hemi ketal SI 5

A round bottom flask was charged with **SI 4** (200 mg, 0.194 mmol, 1 eq). THF: H₂O 2:1 (6.5 mL) was added followed by camphorsulfonic acid (345 mg, 1.49 mmol, 7.7 eq). The reaction was allowed to stir at 23 °C for 3 hours before quenching with triethylamine (414 μL, 2.98 mmol, 15.4 eq). The reaction was dried over sodium sulfate and then concentrated in vacuo. Purification of the resulting residue by flash chromatography (SiO₂: methylene chloride: MeOH 99:1→ 90:10) afforded **SI 5** as a yellow solid (80.9 mg, 0.078 mmol, 40 %).



TLC (methylene chloride: MeOH 9:1)

R_f=0.24, visualized by UV

¹H NMR (750 MHz, pyridine *d*-5: CD₃OD 1:1)

δ 6.70-6.27 (m, 13H), 6.09-6.03 (m, 1H), 5.97-5.90 (m, 1H), 5.65 (app q, J = 6.6 Hz, 1H), 5.52 (app d, J = 17.3 Hz, 1H), 5.46 (dd, J = 10.4 Hz, J = 15.2 Hz, 1H), 5.32 (app dd, J = 1.1 Hz, J = 17.4 Hz, 1H), 5.28 (app d, J = 10.3 Hz, 1H), 5.14 (app d, J = 10.4 Hz, 1H), 4.91-4.86 (m, 1H), 4.77 (s, 1H), 4.76-4.70 (m, 5H), 4.66 (app t, J = 11.0 Hz, 1H), 4.62-4.55 (m, 1H), 4.22 (app d, J = 3.1 Hz, 1H), 4.05 (dd, J = 3.0 Hz, J = -10.2 Hz, 1H), 3.88 (app d, J = 11.1 Hz, 1H), 3.73 (t, J = 9.6 Hz, 1H), 3.65-3.61 (m, 1H), 3.60-3.55 (m, 1H), 3.48-3.45 (m, 1H), 3.34 (app d, J = 9.3 Hz, 1H), 2.62-2.55 (m, 2H), 2.36-2.29 (m, 2H), 2.30-2.16 (m, 3H), 2.06-1.98 (m, 2H), 1.89 (app dd, J = 11.0 Hz, J = 15.2 Hz, 1H), 1.85 (app dd, J = 11.3 Hz, J = 14.3 Hz, 1H), 1.83-1.78 (m, 2H), 1.69 (app dd, J = 2.0 Hz, J = 13.8 Hz, 1H), 1.64-1.52 (m, 4H), 1.48 (d, J = 6.1 Hz, 3H), 1.47-1.39 (m, 3H), 1.37 (d, J = 6.6 Hz, 3H), 1.24 (d, J = 6.4 Hz, 3H), 1.19 (d, J = 7.1 Hz, 3H)

¹³C NMR (125 MHz, acetone *d*-6)

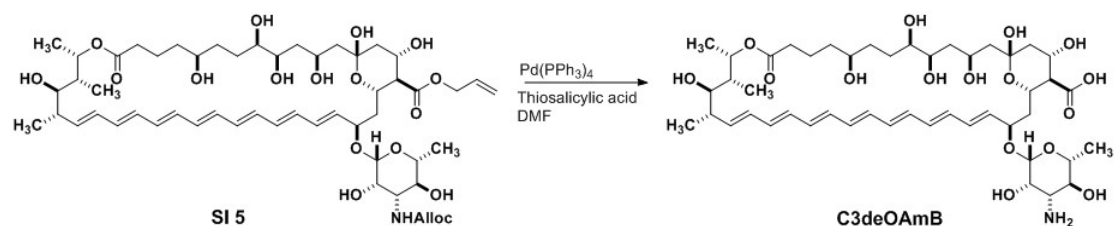
δ 173.2, 172.8, 150.5, 150.3, 150.0, 137.4, 137.0, 134.9, 134.8, 134.6, 134.5, 134.0,

133.8 (3C), 133.7, 133.5 (2C), 133.3, 133.0, 118.2, 117.1, 98.5, 98.4, 98.0, 79.3, 79.1, 77.1, 76.9, 74.4, 70.2, 69.4, 67.0, 66.1, 65.7 (2C), 65.6, 58.6, 58.0, 47.3, 45.5, 43.9, 40.9, 40.8, 39.6, 38.8, 36.5, 35.2, 32.8, 22.8, 18.9, 18.4, 17.1, 12.5

HRMS (ESI)

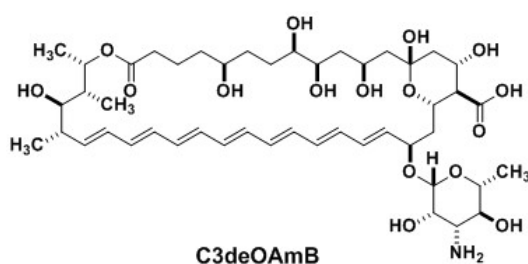
Calculated for $C_{54}H_{81}NO_{18}$ (M+Na)⁺: 1054.5351

Found: 1054.5387



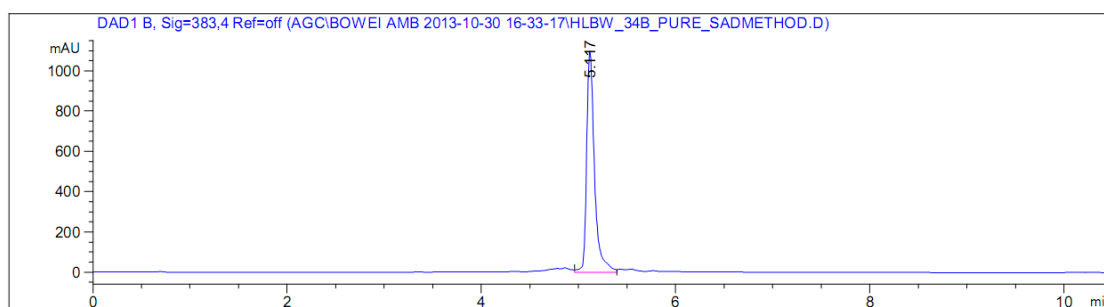
C3deOAmB

A round bottom flask was charged with **SI 5** (35 mg, 0.034 mmol, 1 eq), thiosalicylic acid (26.1 mg, 0.170 mmol, 5 eq) and palladium tetrakis(triphenylphosphine) (11.6 mg, 0.0100 mmol, 0.3 eq). DMF (1.75 mL) was added and the reaction was allowed to stir at 23 °C for 15 minutes before poured into diethyl ether (35 mL). The reaction mixture was then transferred to a 50 mL centrifuge tube and centrifuged at 3700g for 5 minutes. The red pellet was dissolved in DMSO (4 mL) and purified by preparative RP-HPLC (Waters SunFire Prep C₁₈ OBD 5 micron 30 x 150 mm; 25 mL/min flow rate, MeCN: 15 mM NH₄OAc in H₂O 1:19 → 19:1 over 9 minutes, MeCN: 15 mM NH₄OAc in H₂O 19:1 for 1 minute, MeCN: 15 mM NH₄OAc in H₂O 19:1 → 1:19 over 2 minutes) to afford **C3deOAmB** (16.2 mg, 0.018 mmol, 53 %) as a yellow solid.



HPLC (analytical, C₁₈ SiO₂; flow rate = 1.2 mL/min; MeCN: 25 mM NH₄OAc in H₂O 1:19 → 19:1 over 8 minutes)

tR: 5.1 min



^1H NMR (750 MHz, pyridine *d*-5: CD_3OD 1:1)

δ 6.68 (dd, $J = 11.3$ Hz, $J = 14.9$ Hz, 1H), 6.64 (dd, $J = 10.9$ Hz, $J = 14.9$ Hz, 1H), 6.56 (dd, $J = 11.3$ Hz, $J = 14.6$ Hz, 1H), 6.51 (dd, $J = 11.4$ Hz, $J = 13.4$ Hz, 1H), 6.47-6.35 (m, 7H), 6.33-6.25 (m, 2H), 5.69-5.63 (m, 1H), 5.50-5.45 (m, 1H), 5.03 (s, 1H), 4.87 (t, $J = 10.7$ Hz, 1H), 4.79-4.73 (m, 2H), 4.69 (app t, $J = 10.7$ Hz, 1H), 4.57 (app d, $J = 3.2$ Hz, 1H), 3.87 (app d, $J = 11.0$ Hz, 1H), 3.85 (t, $J = 9.8$ Hz, 1H), 3.70-3.68 (m, 2H), 3.65-3.59 (m, 1H), 3.47-3.45 (m, 1H), 3.36-3.31 (m, 1H), 2.82 (app dd, $J = 4.5$ Hz, $J = 15.2$ Hz, 1H), 2.62-2.55 (m, 1H), 2.46 (t, $J = 10.4$ Hz, 1H), 2.34-2.16 (m, 4H), 2.05-1.97 (m, 3H), 1.92-1.86 (m, $J = 9.1$ Hz, $J = 14.0$ Hz, 1H), 1.86-1.78 (m, 2H), 1.66 (app dd, $J = 2.3$ Hz, $J = 13.9$ Hz, 1H), 1.64-1.51 (m, 4H), 1.46 (d, $J = 6.2$ Hz, 3H), 1.45-1.38 (m, 3H), 1.37 (d, $J = 6.5$ Hz, 3H), 1.14 (d, $J = 6.4$ Hz, 3H), 1.19 (d, $J = 7.1$ Hz, 3H)

^{13}C NMR (187.5 MHz, pyridine *d*-5: CD_3OD 1:1)

δ 179.9, 173.6, 137.6, 137.2, 134.8, 134.7, 134.4, 134.1, 134.0, 133.9, 133.8, 133.7, 133.5, 133.0, 130.3, 98.4, 79.3, 78.6, 76.7, 75.1, 74.4, 72.3, 70.6, 70.0, 69.8, 69.1, 67.5, 66.9, 61.5, 57.3, 49.1, 47.8, 45.4, 44.1, 41.2, 40.7, 39.5, 38.9, 36.5, 35.3, 32.2, 30.8, 22.9, 19.1, 18.2, 17.2, 12.7

HRMS (ESI)

Calculated for $\text{C}_{47}\text{H}_{73}\text{NO}_{16}$ ($\text{M}+\text{H}$) $^+$: 908.5008
 Found: 908.5007

III. Planar Lipid Bilayer Experiments

General Information. All data were acquired using a Warner Instruments (Hamden, CT) BC-535 amplifier and the data were filtered using a built in 4 pole Bessel filter with a cutoff frequency of 5 kHz. The headstage and delrin cell were housed within a Warner Instruments model FC-1 Faraday cage. The solutions were stirred using a Warner Instruments SUNstir-3 stirplate. The signal was passed through a Warner Instruments low pass 8 pole Bessel filter with a frequency cutoff of 1 kHz. The filtered data were sampled at a rate of 10 kHz using a Molecular Devices (Sunnyvale, CA) Digidata 1440 data acquisition system and the data were analyzed using Molecular Devices pClamp 10 software. Salt bridges were prepared monthly and were fabricated from 1.5 mm OD, 0.86 mm ID borosilicate capillary tubing and were filled with 1 M aqueous KCl with 2.5 % agar. Prior to a day's experiments, silver electrodes were plated by submerging in commercial bleach for 15 to 30 minutes. The electrodes were plated periodically throughout the day.

Preparation of Lipid Solution. Lipids were obtained from Avanti Polar Lipids as 10 mg/mL solutions in CHCl_3 . The solutions were stored at $-20\text{ }^\circ\text{C}$ under dry argon and used within 3 months. A 4 mg/mL solution of ergosterol in CHCl_3 was prepared monthly and stored at $-20\text{ }^\circ\text{C}$ under dry argon. Lipid films were prepared by charging a 1.5 mL vial with 60 μL DPhPC, and 30 μL ergosterol. The solvent was removed with a gentle stream of nitrogen. The lipid film was then dissolved in 30 μL n-decane to give the 20 mg/mL solution of lipids used for the electrophysiology experiments. The decane solutions were used within 3 hours of preparation.

Formation of planar lipid bilayers. Custom manufactured polysulfone cups were machined with a 150 μm aperture (modeled after Warner Instruments model 64-0416, Hamden, CT). The area around the hole was then primed with 1 μL of the decane lipid solution. The primed cup was left to stand for approximately 10 minutes such that most of the decane evaporated. Then 1 mL of a 1 M KCl, 5 mM HEPES at $\text{pH} = 7.0$ was added to each chamber. The membrane was formed by sequential vertical swabs across the hole using a flame polished glass applicator that had been previously dipped into the lipid solution. The formation of a membrane was detected by a reduction in the current to 0 pA. The integrity of this membrane was confirmed by applying a potential of 150 mV for approximately one minute. If the current increased by >1 pA upon voltage introduction, the membrane was rejected. Membranes were between 45 and 105 pF in size.

Interrogating Channel Formation. If the membrane was acceptable, 0.25 - 1 μL of a compound in DMSO was added to both chambers and the solutions were stirred with zero applied potential for 3 minutes. After 3 minutes the stirring was stopped, and a potential was applied across the membrane. The formation of single AmB channels under similar conditions has been well documented.³ The concentration of AmB and C3deOAmB required to observe channel activity varied from membrane to membrane and appeared to depend on the membrane capacitance. For both AmB and C3deOAmB, single channel formation was observed at concentrations between 0.25 and 5 nM.

A standardized protocol was used to perform these experiments with both AmB and C3deOAmB. Each compound was initially added to both sides of the lipid bilayer at 0.5 nM and then channel activity was investigated for 10 minutes. If no channel activity was observed, a small amount of additional compound was added to both sides of the membrane to increase the concentration by 0.5 nM and then channel activity was investigated for 10 minutes again. This process was repeated until single channel activity was observed, or until we reached a concentration of 5 nM, observed multi-channel formation (data not used) or observed membrane rupture. For both AmB and C3deOAmB, single channel data were typically recorded at 0.5 nM.

To measure conductance of AmB and C3deOAmB the same basic experimental setup was used with the following slight modifications. A 2 M KCl, 5 mM HEPES $\text{pH} = 7.0$ bathing solution was used instead of the 1 M KCl, 5 mM HEPES $\text{pH} = 7.0$ solution. Upon bilayer formation and addition of compound to both sides of the membrane channel activity was investigated at 90, 120, 150, 180, and 210 mV applied potential.

Single Channel Characterization. All data processing was performed within the pClamp v10 software suite. Following acquisition, the data was digitally filtered to 20 Hz. Then using the single channel search feature (ignore short level changes of 40 ms or less, update baseline automatically) the amplitude of the open and closed states was determined. The delta between the open and closed levels represents the single channel current at the given applied voltage. Dwell times were calculated from single ion channel traces.

Best-fit lines of the current vs. voltage plot of both AmB and C3deOAmB single ion channels were determined via linear regression. The slope is equal to the conductance of the corresponding channel based on Ohm's Law. Errors were determined from the standard error of the linear regression. The p value of equivalent AmB and C3deOAmB single ion channel conductances was calculated to be less than 0.0001.

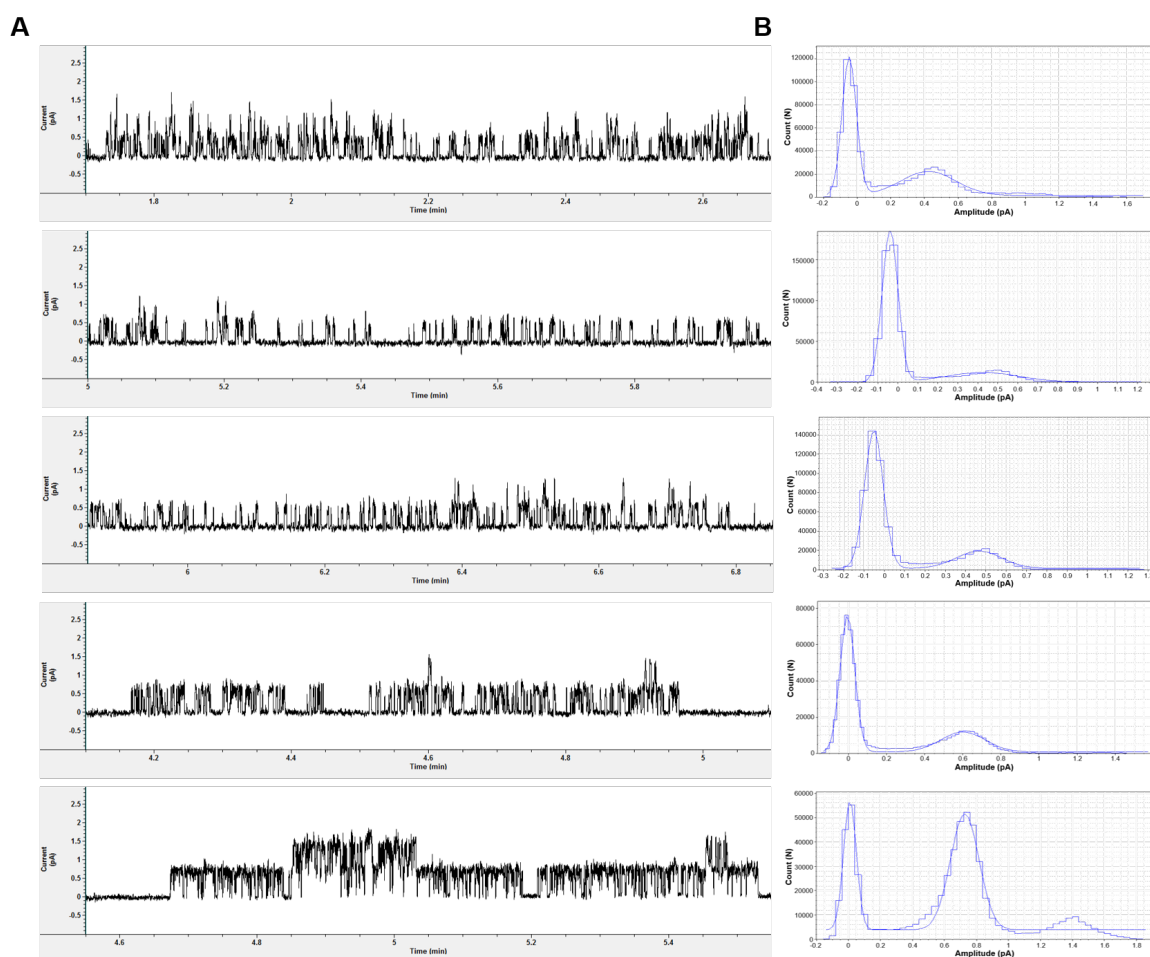


Figure S1: A.) Representative traces of AmB single ion channel activity in planar lipids bilayers. DPhPC Lipids with 30% Ergosterol. 1 M KCl pH = 7.0, 5 mM HEPES +150 mV. Each representative trace contains one minute of recording. B.) Corresponding amplitude diagrams with Gaussian fits for each of the AmB single ion channel traces. Average dwell times for AmB single ion channel activity were 135.2 ± 65.03 ms.

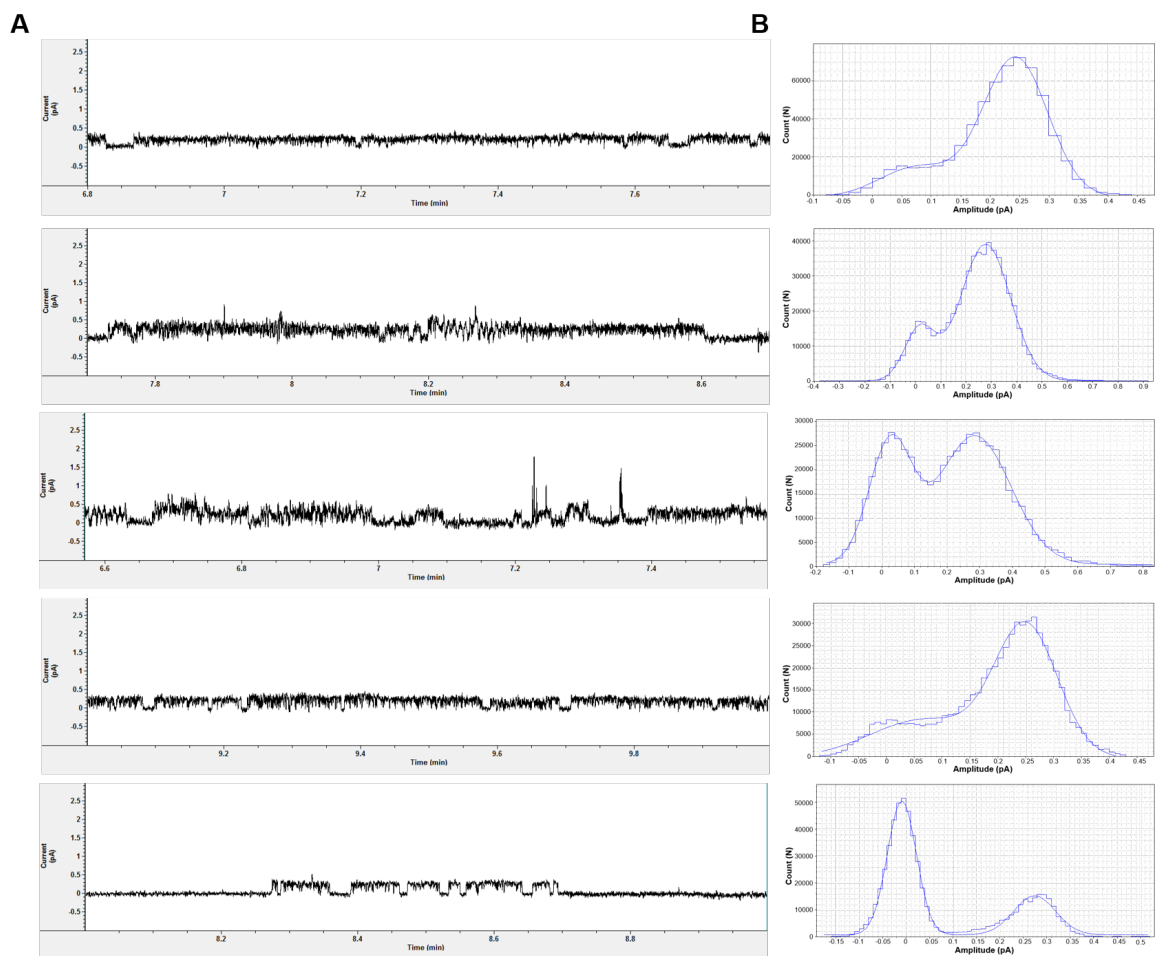


Figure S2: A.) Representative traces of C3deOAmB single ion channel activity in planar lipids bilayers. DPhPC Lipids with 30% Ergosterol. 1 M KCl pH = 7.0, 5 mM HEPES +150 mV. Each representative trace contains one minute of recording. B.) Corresponding amplitude diagrams with Gaussian fits for each of the C3deOAmB single ion channel traces. Average dwell times for C3deOAmB single ion channel activity were 1265 ± 363.1 ms.

IV. Liposome Efflux Experiments

General Information. Potassium selective measurements were obtained using a Denver Instruments (Denver, CO) Model 225 pH meter equipped with a World Precision Instruments (Sarasota, FL) potassium selective electrode inside a Faraday cage. The electrode was filled with 1000 ppm KCl standard solution and conditioned in a 1000 ppm KCl standard solution for 15 minutes prior to potassium selective measurements. Measurements were made on 3 mL solutions that were magnetically stirred in 7 mL vials incubated at 23 °C. The instrument was calibrated daily with KCl standard solutions to 10, 100, and 1000 ppm potassium. The potassium concentration was sampled every 10 seconds throughout the course of the efflux experiments. Proton selective measurements were obtained using a Fisher Scientific (Hampton, NH) micro pH electrode. Measurements were made on 3 mL solutions that were magnetically stirred in 7 mL vials incubated at 23 °C. The instrument was calibrated daily with pH standard solutions of 4, 7, and 10. The pH was sampled every 30 seconds throughout the course of the efflux experiments.

Liposome preparation. Palmitoyl oleoyl phosphatidylcholine (POPC) was obtained as a 25 mg/mL solution in CHCl_3 from Avanti Polar Lipids (Alabaster, AL) and was stored at -20 °C under an atmosphere of dry argon and used within 3 months. A 4 mg/mL solution of ergosterol in CHCl_3 was prepared monthly and stored at 4 °C under an atmosphere of dry argon. Prior to preparing a lipid film, the solutions were warmed to ambient temperature to prevent condensation from contaminating the solutions. A 7 mL vial was charged with 640 μL POPC and 230 μL of the ergosterol solution. The solvent was removed with a gentle stream of nitrogen and the resulting lipid film was stored under high vacuum for a minimum of eight hours prior to use. For potassium efflux experiments, the film was then hydrated with 1 mL of 150 mM KCl, 5 mM HEPES buffer pH 7.4 and vortexed vigorously for approximately 3 minutes to form a suspension of multilamellar vesicles (MLVs). For proton efflux experiments, the film was hydrated with 1 mL of 400 mM Sodium Phosphate buffer pH 5.5. The resulting lipid suspension was pulled into a Hamilton (Reno, NV) 1 mL gastight syringe and the syringe was placed in an Avanti Polar Lipids Mini-Extruder. The lipid solution was then passed through a 0.20 μm Millipore (Billerica, MA) polycarbonate filter 21 times, the newly formed large unilamellar vesicle (LUV) suspension being collected in the syringe that did not contain the original suspension of MLVs to prevent the carryover of MLVs into the LUV solution. To obtain a sufficient quantity of LUVs, three independent 1 mL preparations were pooled together for the dialysis and subsequent efflux experiments. The newly formed LUVs were dialyzed using Pierce (Rockford, IL) Slide-A-Lyzer MWCO 3,500 dialysis cassettes. For potassium efflux experiments, the samples were dialyzed three times against 600 mL of 150 mM NaCl, 5 mM HEPES buffer pH 7.4. For proton efflux experiments, the samples were dialyzed three times against 600 mL of 400 mM Sodium Sulfate pH 7.5. The first two dialyses were two hours long, while the final dialysis was performed overnight.

Determination of Phosphorus Content. Determination of total phosphorus was adapted from the report of Chen and coworkers.⁴ The LUV solution was diluted tenfold with either 150 mM NaCl, 5 mM HEPES buffer pH 7.4 (potassium efflux experiments) or 400 mM Sodium Sulfate pH 7.5 (proton efflux experiments). Three 10 μL samples of the diluted LUV suspension were added to three separate 7 mL vials. Subsequently, the solvent was removed with a stream of N_2 . To each

dried LUV film, including a fourth vial containing no lipids that was used as a blank, was added 450 μL of 8.9 M H_2SO_4 . The four samples were incubated open to ambient atmosphere in a 225 $^\circ\text{C}$ aluminum heating block for 25 min and then removed to 23 $^\circ\text{C}$ and cooled for 5 minutes. After cooling, 150 μL of 30% w/v aqueous hydrogen peroxide was added to each sample, and the vials were returned to the 225 $^\circ\text{C}$ heating block for 30 minutes. The samples were then removed to 23 $^\circ\text{C}$ and cooled for 5 minutes before the addition of 3.9 mL water. Then 500 μL of 2.5% w/v ammonium molybdate was added to each vial and the resulting mixtures were then vortexed briefly and vigorously five times. Subsequently, 500 μL of 10% w/v ascorbic acid was added to each vial and the resulting mixtures were then vortexed briefly and vigorously five times. The vials were enclosed with a PTFE lined cap and then placed in a 100 $^\circ\text{C}$ aluminum heating block for 7 minutes. The samples were removed to 23 $^\circ\text{C}$ and cooled for approximately 15 minutes prior to analysis by UV/Vis spectroscopy. Total phosphorus was determined by observing the absorbance at 820 nm and comparing this value to a standard curve obtained through this method and a standard phosphorus solution of known concentration.

Efflux from LUVs. The LUV solutions were adjusted to 1 mM using either 150 mM NaCl, 5 mM HEPES buffer pH 7.4 (potassium efflux experiments) or 400 mM Sodium Sulfate pH 7.5 (proton efflux experiments). 3 mL of the 1 mM LUV suspension was added to a 7 mL vial, and the solution was gently stirred. The appropriate probe was inserted, and data were collected for one minute prior to addition of compound. Then 30 μL of a 0.1 mM DMSO solution of the compound was added, and data were collected until there was no change in efflux for at least 3 data points. To effect complete ion release, 30 μL of a 10% v/v solution of triton X-100 was added, and data were collected for an additional five minutes.

Data Analysis. The data from each run was normalized to the percent of total ion release from 0 to 100%. Thus for each experiment a scaling factor S was calculated. For example, the scaling factor for potassium efflux was calculated using the following relationship:

$$\left[\frac{[\text{K}^+]_{final}}{[\text{K}^+]_{initial}} - 1 \right] \cdot S = 100$$

Each concentration data point was then multiplied by S before plotting as a function of time. To calculate half-life (time to reach half of the maximum efflux), each efflux experiment was plotted in Origin Pro and fitted using an exponential decay function.

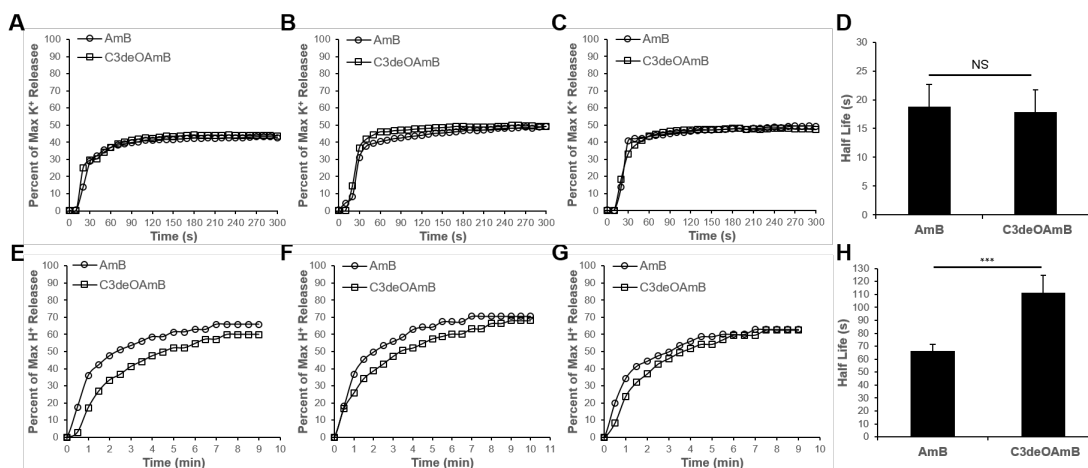


Figure S3: A.-C.) Potassium efflux experiments with either 1 μM AmB or C3deOAmB. D.) Average half-lives calculated using exponential decay fitting from potassium efflux experiments. E.-G.) Proton efflux experiments with either 1 μM AmB or C3deOAmB. H.) Average half-lives calculated using exponential decay fitting from proton efflux experiments. DMSO vehicle was performed in triplicate and subtracted from AmB and C3deOAmB experiments to account for instrumental drift. $N \geq 5$ for all experiments. Graphs depict means \pm SD. NS, not significant. *** $p < 0.01$.

Part B

I. NMR studies

H-H NOESY NMR Spectra. 750 MHz spectra were acquired at room temperature with 2218 points, 512 increments, and 64 transients per increment. Spectra were processed using nmrPipe⁵ as follows: the Sparky program⁶ was used for peak-picking and integration of crosspeaks (see Table S2). The following formula was used to convert peak intensity to distance:

$$r_x = \left(\frac{V_x}{V_{std}} \right)^{-1/6} * r_{std}$$

where r_{std} and V_{std} are based off of the integration values for H31-H33 proton – proton distance.

Phase-Sensitive COSY (COSYPS) NMR Spectra. 750 MHz spectra were acquired at room temperature with 2218 points, 720 increments, and 16 transients per increment. Spectra were processed using nmrPipe⁵ as described by Delagio et al.⁷ All COSYPS spectra were acquired with sufficient interscan delay to allow for full spin-relaxation ($d1 = 10$ seconds for AmB and 15 for C3deOAmB, as determined by T1 relaxation experiments).

HSQC. A gradient HSQC spectrum was acquired at room temperature on a 750 MHz spectrometer with 2218 points, 512 increments, and 8 transients per increment.

COSYPS processing and ³J determination. Raw COSYPS data were processed as described by Delagio et al.⁷ to produce a diagonal-suppressed spectrum and a diagonal-only spectrum.

Amplitude-constrained multiplet evaluation (ACME)⁷ was used to determine the ³J H-H coupling constants (see Table S1 for all coupling constants calculated by ACME).

Crosspeak Fitting. The ACME method for determining J values from the COSYPS spectra is described at length by Delagio et al.⁷ The values are determined as described by Palacios et al.⁸

Dihedral angles are calculated from the ³J H-H coupling constants generated by the ACME program using the MestReJ software.⁹ Each ³J H-H constant will yield 4 possible solutions to the Karplus equation. The angle chosen was consistent with the angles of the crystal structure. The selected dihedral angles ($\pm 30^\circ$) were used as restraints in LowModeMD conformational searches (see Section II).

II. Computational Conformational Search with Energy Minimization Calculations

LowModeMD conformational searches¹⁰ were performed using the Molecular Operating Environment suite (MOE), Version 2014.09,¹¹ with the empirical MMFF94x force field and a distance solvation model. In brief, conformations were perturbed along a molecular dynamics trajectory, with kinetic energy variations in the low frequency vibrational modes, followed by energy minimization.¹⁰ Initial atomic coordinates and structure files for both AmB and C3deOAmB were generated from the AmB crystal structure (CCDC 866798)¹² using MOE. NMR-derived distance and dihedral angle restraints were applied with weight factors of 2 kcal/mol/Å and 0.02 kcal/mol/deg, respectively. The conformational searches were performed with an iteration limit of 10,000 and a rejection limit up to 500. Default values were used for all other parameters.

Each H-C-C-H dihedral angle was restrained to the selected value $\pm 30^\circ$ (see Table S1). Consistent with the standard convention for dihedral angles, dihedral angle values were defined using the following range, $-180^\circ < \theta \leq 180^\circ$. The π -bonds in the polyene moiety were constrained to $180 \pm 10^\circ$.

Interproton distances were restrained for proton pairs exhibiting NOE correlations, with the lower limit set at 1.8 Å and the upper limit set at 2.5 Å, 3.5 Å, or 5.0 Å for strong, medium, and weak correlations, respectively (see Table S2). In the case of a proton pairing with a proton from a methyl group, that proton-proton distance was defined between the proton and the carbon atom of the methyl group with an expanded distance range, and weighted half as much.

The top conformers for both AmB and C3deOAmB were imported into VMD¹³ and aligned using the RMSD Calculator Tool. Only the heavy atoms pictured below were used for the alignment and RMSD calculation.

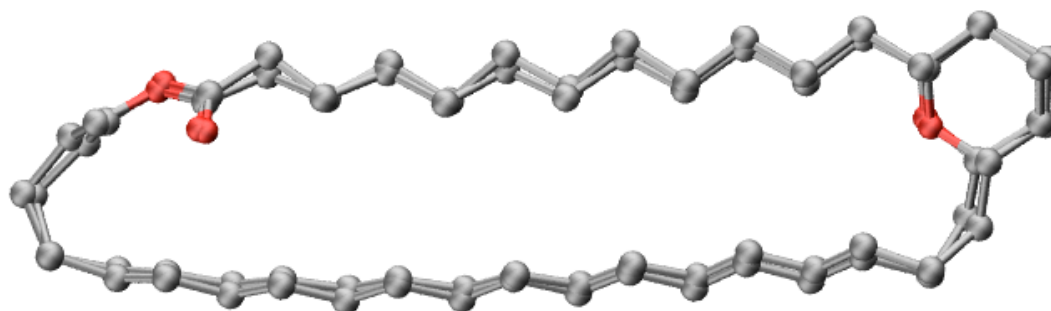


Figure S4: Structure-based alignment of the lowest energy conformation of the AmB skeleton with the crystal structure. RMSD of the best conformer is 0.2868 ± 0.0005 Å.

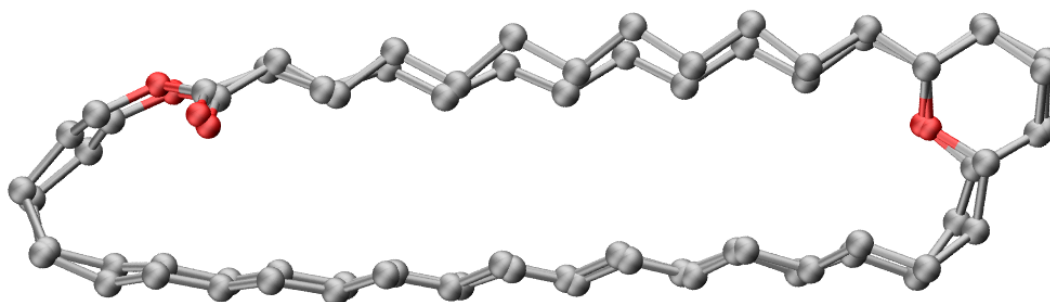


Figure S5: Structure-based alignment of the lowest energy conformation of the C3deOAmB skeleton with the crystal structure. RMSD of best conformer is 0.55 ± 0.02 Å.

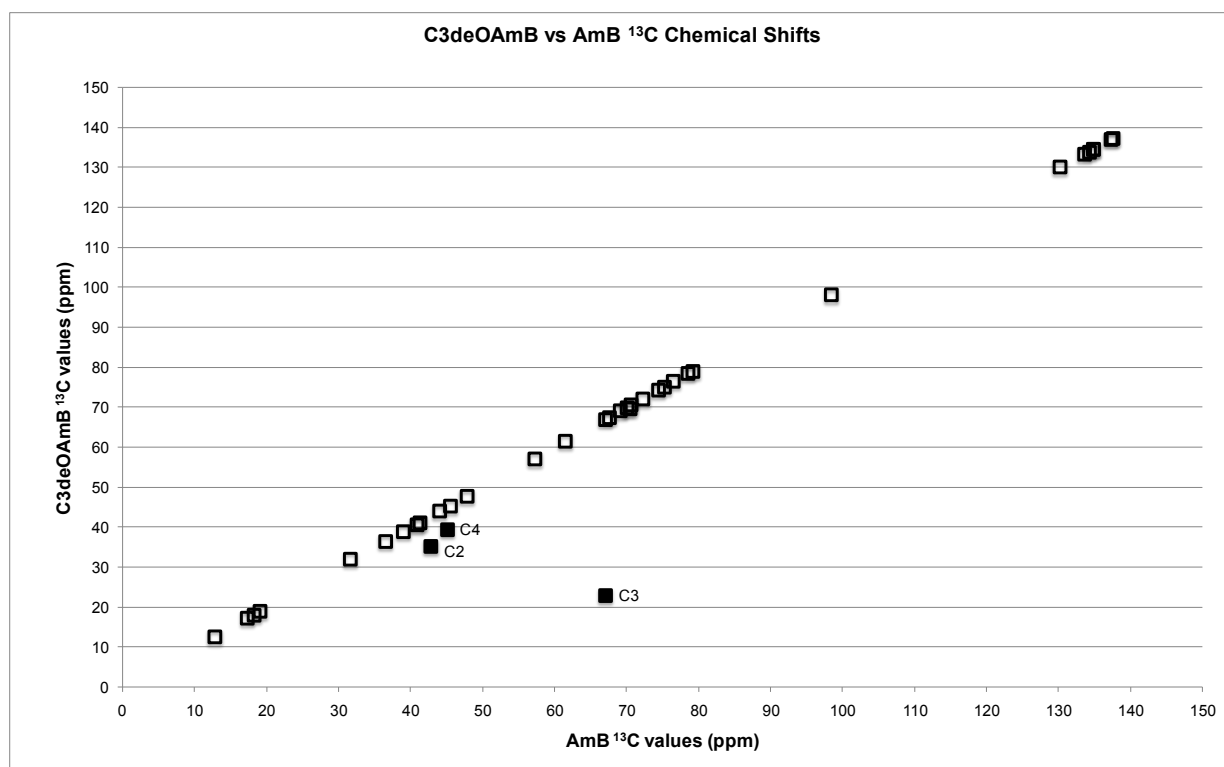


Figure S6: Plot of ^{13}C chemical shifts for C3deOAmB versus AmB molecule. The outliers are C2, C4 and C3.

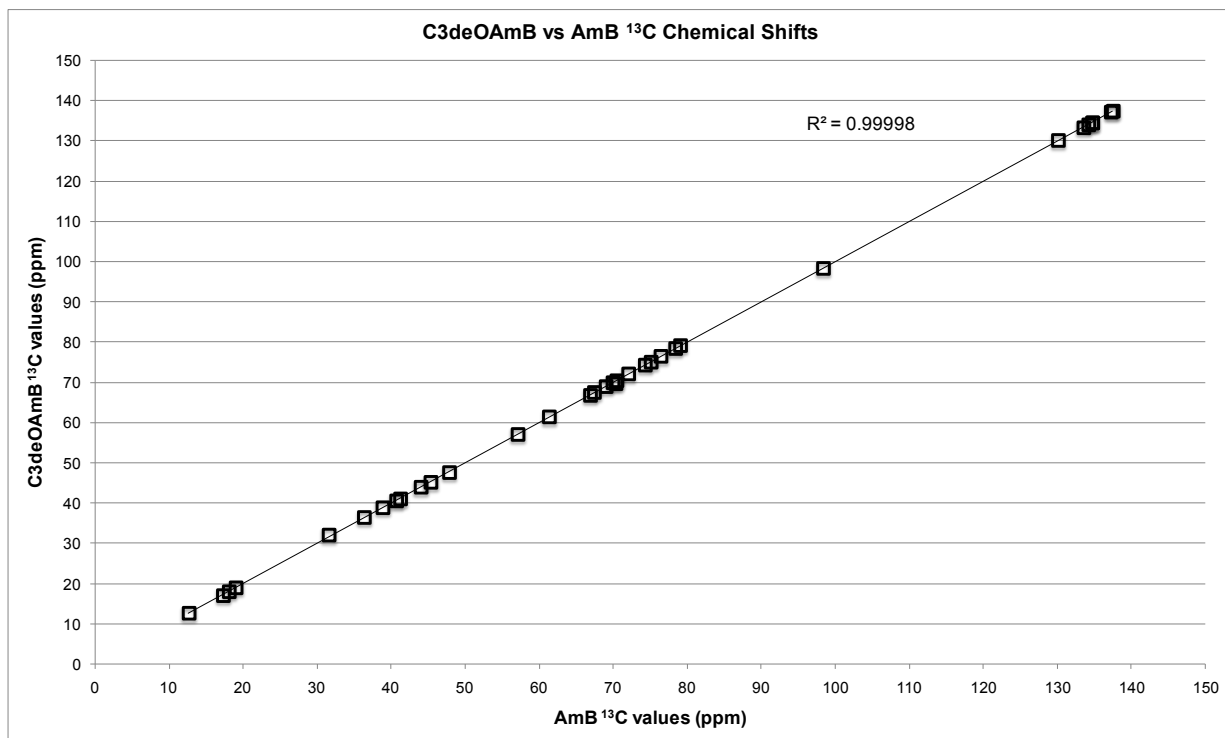


Figure S7: Plot of ¹³C chemical shift values for C3deOAmB versus AmB molecule with the outliers C2, C3 and C4 removed. R^2 is 0.99998.

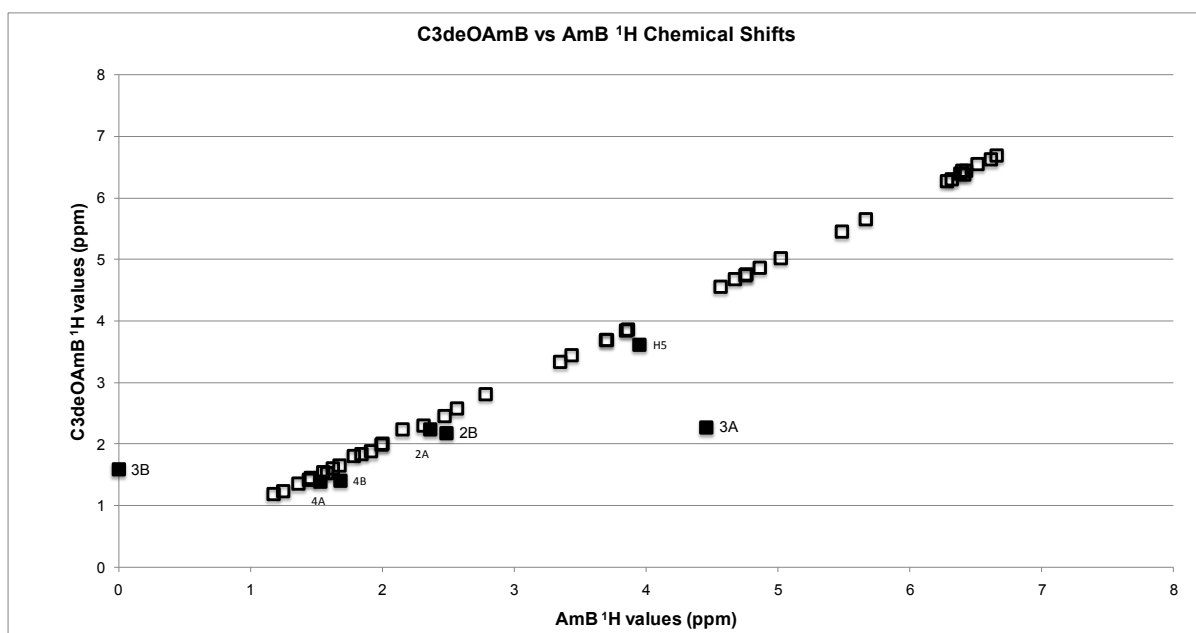


Figure S8: Plot of ¹H chemical shifts for C3deOAmB versus AmB molecule. The outliers are H2A, H2B, H3A, H3B, H4A, H4B, H5.

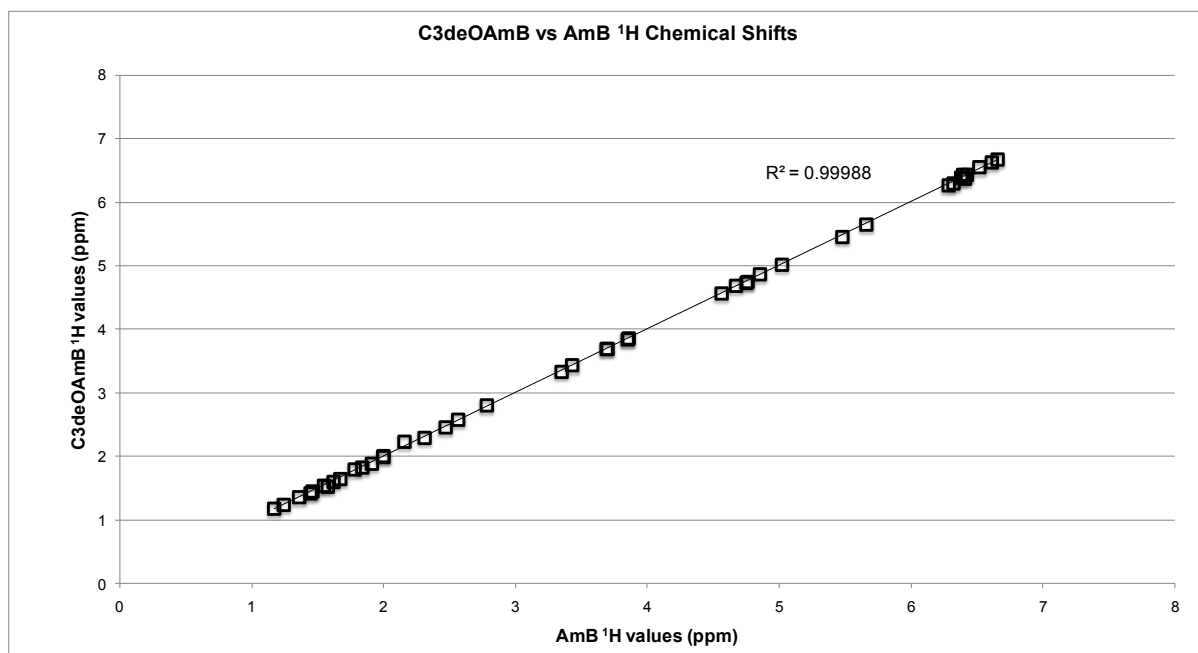


Figure S9: Plot of ¹H chemical shift values for C3deOAmB versus AmB molecule with the outliers H2A – H5 removed. R² is 0.99988.

Table S1: Coupling constants yielded from ACME analysis and the corresponding dihedral values for both AmB and C3deOAmB. The dihedral angles of the crystal structure are also listed for comparison.

Proton	AmB	C3deOAmB	Protons	AmB	C3deOAmB
	<i>J</i> (Hz)	<i>J</i> (Hz)		θ (°)	θ (°)
2a-2b	16.3	8.1	2a-2b	NA	NA
2a-3a	3.4	ND	2a-3a	-62	ND
2a-3b	NA	8.8	2a-3b	NA	148
2b-3a	10.1	ND	2b-3a	155	ND
2b-3b	NA	ND	2b-3b	NA	ND
3a-3b	NA	14.4	3a-3b	NA	NA
3a-4a	3.3	8.2	3a-4a	62	41
3a-4b	9.9	8.2	3a-4b	-154	-145
3b-4a	NA	4.7	3b-4a	NA	-129
3b-4b	NA	9.3	3b-4b	NA	-37
4a-4b	13.8	ND	4a-4b	NA	NA
4a-5	3.2	6.8	4a-5	-63	-47
4b-5	9.6	6.8	4b-5	-152	-139
5-6a	1.8	ND	5-6a	70	ND
5-6b	10.2	10.8	5-6b	156	160
6a-6b	11.4	13.0	6a-6b	NA	NA
6b-7b	ND	2.9	6b-7b	ND	64
6b-7a	5.7	8.9	6b-7a	-134	-149
6a-7a	5.2	4.1	6a-7a	-54	-59
6a-7b	ND	8.8	6a-7b	ND	-148
7a-7b	11.6	12.7	7a-7b	NA	NA
7a-8	ND	ND	7a-8	ND	ND
7b-8	10.4	ND	7b-8	-157	ND
8-9	ND	ND	8-9	ND	ND
9-10a	2.0	2.1	9-10a	69	69
9-10b	11.0	11.0	9-10b	-161	-161
10a-10b	13.9	14.0	10a-10b	NA	NA
10a-11	3.0	2.1	10a-11	-64	-69
10b-11	10.2	10.0	10b-11	-156	-155
11-12a	2.2	1.7	11-12a	68	71
11-12b	11.0	11.2	11-12b	161	163
12a-12b	13.8	13.8	12a-12b	NA	NA
14a-14b	11.2	12.1	14a-14b	NA	NA
14a-15	11.4	11.5	14a-15	164	165
14b-15	4.9	5.0	14b-15	55	55
15-16	9.9	10.4	15-16	-154	-157
16-17	10.4	10.8	16-17	-157	-160
17-18a	ND	ND	17-18a	ND	ND
17-18b	8.1	8.8	17-18b	145	148
18a-18b	14.5	14.6	18a-18b	NA	NA
18b-19	2.0	2.2	18b-19	69	68
18a-19	4.5	4.2	18a-19	-57	-58
19-20	9.2	9.4	19-20	150	151
20-21	15.5	15.3	20-21	180	180
21-22	11.1	11.3	21-22	-151	-152
22-23	15.1	14.8	22-23	180	180
23-24	8.2	ND	23-24	139	ND
24-25	15.1	ND	24-25	180	180
25-26	ND	ND	25-26	ND	ND
26-27	ND	ND	26-27	-180	-180
27-28	ND	ND	27-28	ND	ND
28-29	ND	ND	28-29	180	180
29-30	ND	ND	29-30	ND	ND
30-31	ND	ND	30-31	-180	-180
31-32	ND	ND	31-32	ND	ND
32-33	15.3	14.7	32-33	-180	-180
33-34	11.5	10.9	33-34	153	150
34-35	9.8	9.8	34-35	-145	-145
35-36	2.2	2.2	35-36	-72	-72
36-37	1.2	1.2	36-37	-72	-72
1'-2'	1.2	1.1	1'-2'	75	75
2'-3'	3.1	3.1	2'-3'	-63	-63
3'-4'	10.4	10.4	3'-4'	157	157
4'-5'	10.0	9.6	4'-5'	-155	-152
37-38	7.1	7.1	37-38	NA	NA
36-39	7.0	7.2	36-39	NA	NA
34-40	7.2	7.0	34-40	NA	NA

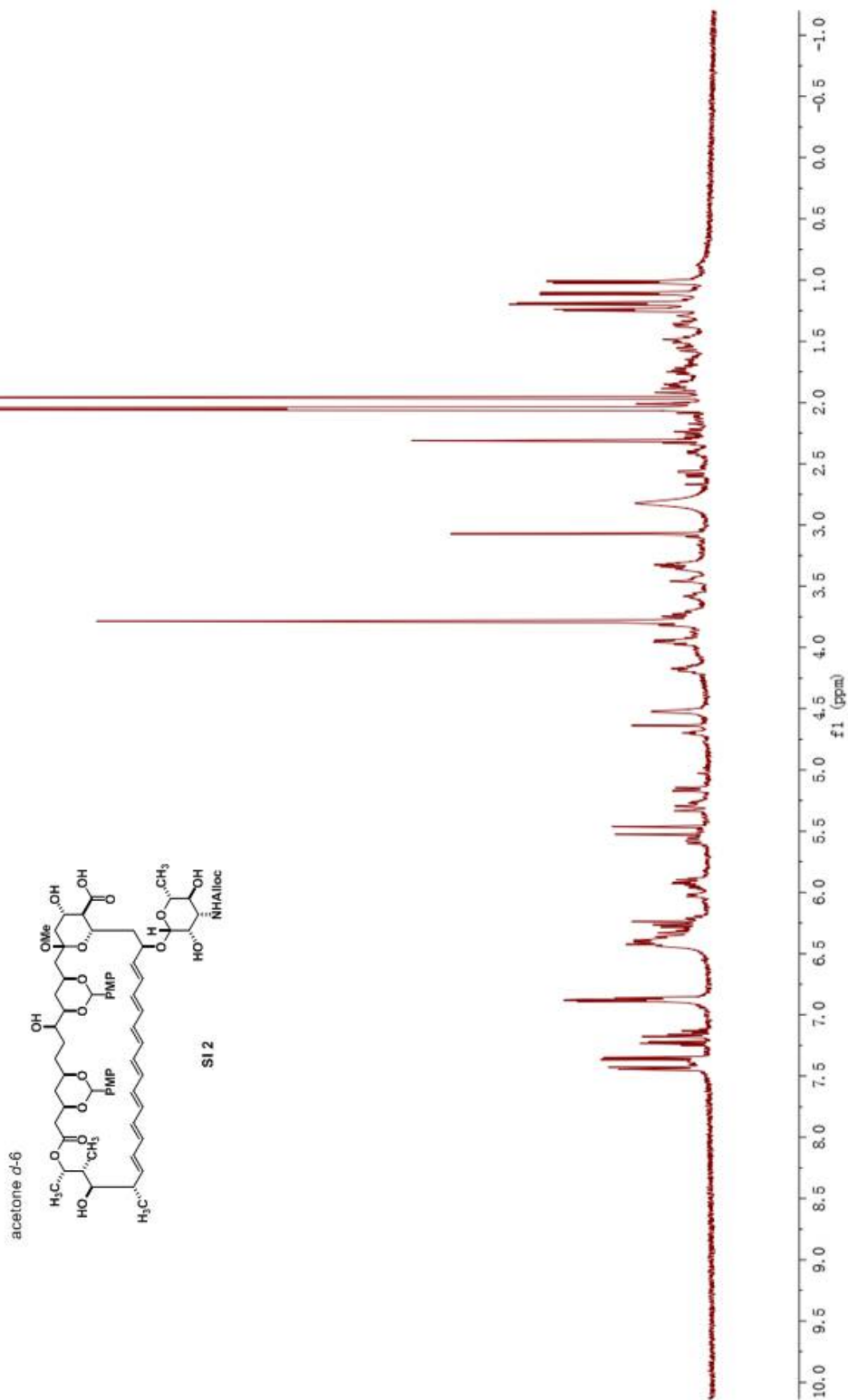
Table S2: NOESY distances for both AmB and C3deOAmB. Peak intensities greater than $2 * 10^8 \text{ \AA}^3$ were categorized as strong correlations, between $2.7 * 10^7$ and $2 * 10^8 \text{ \AA}^3$ were categorized as medium and anything under $2.7 * 10^7 \text{ \AA}^3$ was categorized as a weak NOESY correlation.

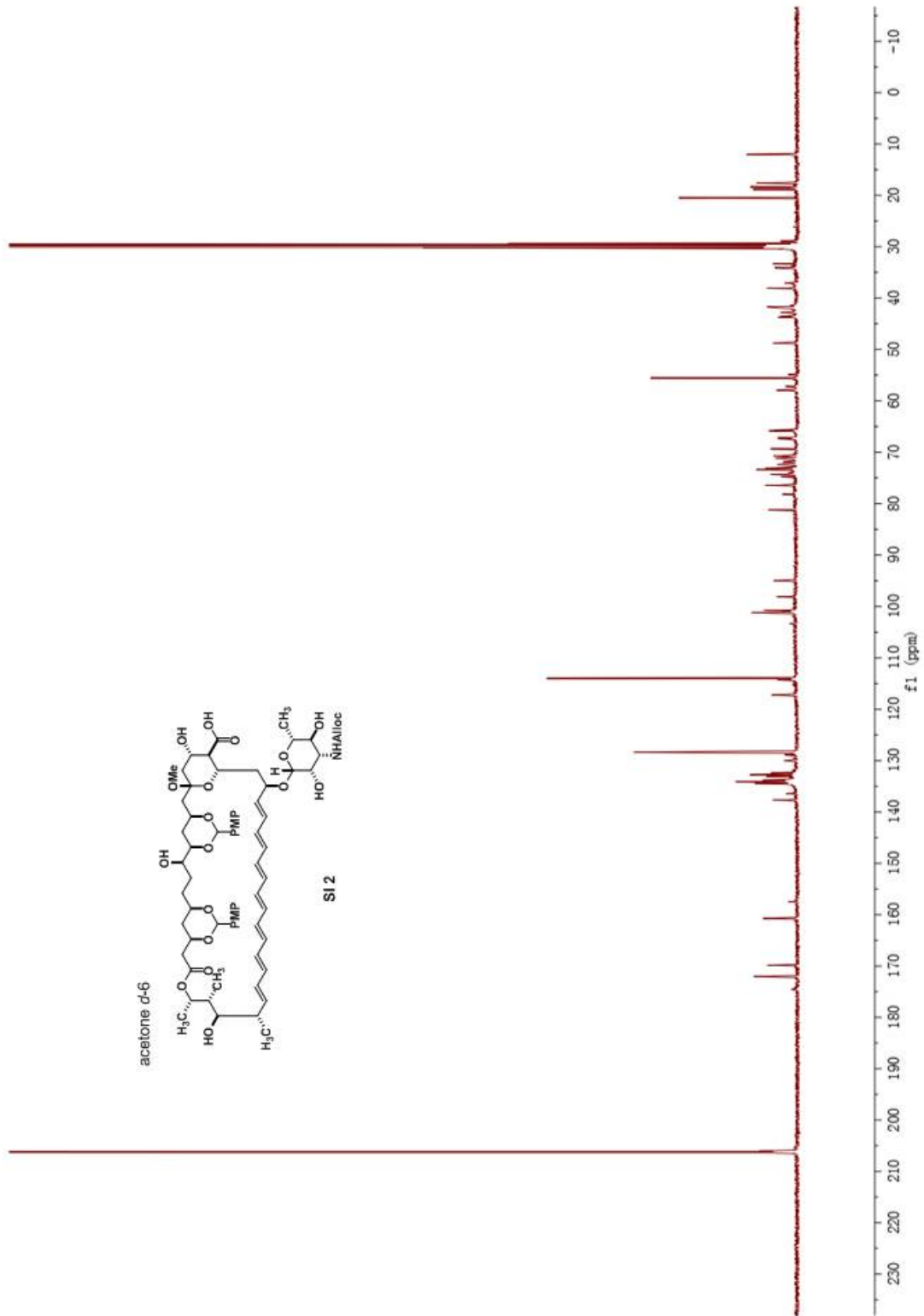
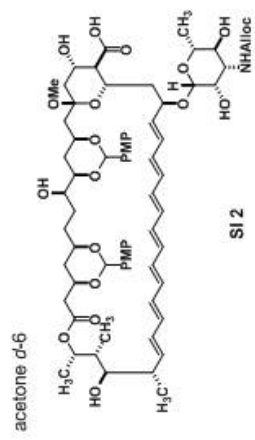
	AmB Proton Pair	Peak Intensity (Vx)	C3deOAmB Proton Pair	Peak Intensity (Vx)
1	AmBH2a-H2b	5.2E+08		
2	AmBH2a-H3	4.7E+07		
3	AmBH2a-H4a	3.8E+07		
4	AmBH2a-H4b	8.8E+07		
5	AmBH2a-H5	1.1E+07		
6	AmBH2a-H25	1.5E+07		
7	AmBH2a-H36	1.1E+07		
8	AmBH2a-H37	5.5E+06	C3AmBH2a-H37	6.6E+06
9	AmBH2a-H38	6.1E+06		
10	AmBH2a-H39	6.0E+06	C3AmBH39-H2a	3.8E+06
11	AmBH2b-H3	2.7E+07		
12	AmBH2b-H4a	8.1E+07		
13	AmBH2b-H4b	4.6E+07		
14	AmBH2b-H5	6.4E+06		
15	AmBH2b-H37	6.4E+06	C3AmBH2b-H37	9.4E+06
16	AmBH2b-H38	9.8E+06		
17	AmBH2b-H39	5.0E+06	C3AmBH39-H2b	7.7E+06
18			C3AmBH3a-H3b	4.9E+08
19	AmBH3-H4a	2.5E+07		
20	AmBH3-H4b	4.6E+07		
21	AmBH3-H5	9.5E+07	C3AmBH3a-H5	9.0E+07
22	AmBH3-H6a	4.2E+06		
23	AmBH3-H6b	1.7E+07		
24	AmBH3-H7a	6.0E+06		
25	AmBH3-H7b	7.6E+06		
26	AmBH3-H25	5.0E+07		
27	AmBH3-H26	4.7E+06		
28	AmBH3-H37	3.3E+06	C3AmBH3a-H37	7.3E+06
29	AmBH3-H38	4.6E+06		
30	AmBH3-H39	4.2E+06		
31			C3AmBH3b-H31	1.0E+07
32			C3AmBH3b-H32	6.9E+07
33	AmBH4a-H4b	3.5E+08		
34	AmBH4a-H5	2.4E+07	C3AmBH4a-H5	1.1E+08
35	AmBH4a-H6a	2.0E+08		
36	AmBH4a-H7a	1.1E+07		
37	AmBH4b-H5	4.3E+07	C3AmBH4b-H5	8.4E+07
38	AmBH4b-H6a	6.0E+07		
39	AmBH4b-H7a	1.5E+07		
40	AmBH4b-H8	5.7E+06		
41	AmBH4b-H25	1.4E+07		
42	AmBH5-H6a	1.7E+07	C3AmBH5-H6a	4.6E+07
43	AmBH5-H6b	3.9E+07	C3AmBH5-H6b	1.2E+08
44	AmBH5-H7a	3.0E+07	C3AmBH5-H7a	1.1E+08
45	AmBH5-H7b	5.5E+07	C3AmBH5-H7b	3.3E+08
46	AmBH5-H8	1.4E+07	C3AmBH8-H5	2.0E+07
47	AmBH5-H22	4.5E+06		
48			C3AmBH5-H24	1.2E+07
49	AmBH5-H25	4.9E+07	C3AmBH5-H25	2.5E+07
50	AmBH5-H26	2.5E+07	C3AmBH5-H26	5.5E+07
51			C3AmBH5-H32	2.7E+07
52	AmBH6a-H6b	3.6E+08	C3AmBH6a-H6b	5.7E+08
53	AmBH6a-H7a	7.7E+07	C3AmBH6a-H7a	1.6E+08
54	AmBH6a-H7b	9.4E+07		
55				
56	AmBH8-H6a	5.6E+07	C3AmBH6a-H8	9.2E+07
57	AmBH6a-H9	8.3E+06		
58	AmBH6b-H7a	8.4E+07		
59	AmBH6b-H8	5.3E+07	C3AmBH6b-H8	1.5E+08
60	AmBH6b-H11	1.4E+07		
61	AmBH6b-H9	1.6E+07	C3AmBH6b-H9	3.8E+07
62	AmBH6b-H24	4.4E+06		
63	AmBH6b-H25	1.1E+07		
64	AmBH6b-H26	7.4E+06		
65	AmBH7a-H7b	3.6E+08	C3AmBH7a-H7b	8.5E+08
66	AmBH7a-H8	3.1E+07	C3AmBH8-H7a	6.3E+07
67	AmBH7a-H9	3.5E+07	C3AmBH7a-H9	8.0E+07
68	AmBH7a-H10a	4.0E+07	C3AmBH7a-H10a	4.6E+07
69	AmBH7a-H10b	1.7E+07		
70			C3AmBH7a-H11	1.4E+07
71	AmBH7a-H22	5.2E+06		
72			C3AmBH7a-H24	3.2E+07
73	AmBH7b-H24	2.7E+07	C3AmBH7b-H24	6.0E+07
74	AmBH7a-H25	1.3E+07		
75	AmBH7a-H26	1.7E+07	C3AmBH7a-H26	3.3E+07
76	AmBH7b-H8	8.7E+07	C3AmBH7b-H8	1.3E+08
77	AmBH7b-H9	9.3E+07	C3AmBH7b-H9	2.1E+08
78	AmBH7b-H10a	3.7E+07	C3AmBH7b-H10a	2.7E+07
79	AmBH7b-H11	1.2E+07	C3AmBH7b-H11	2.0E+07
80	AmBH22-H7b	1.2E+07		

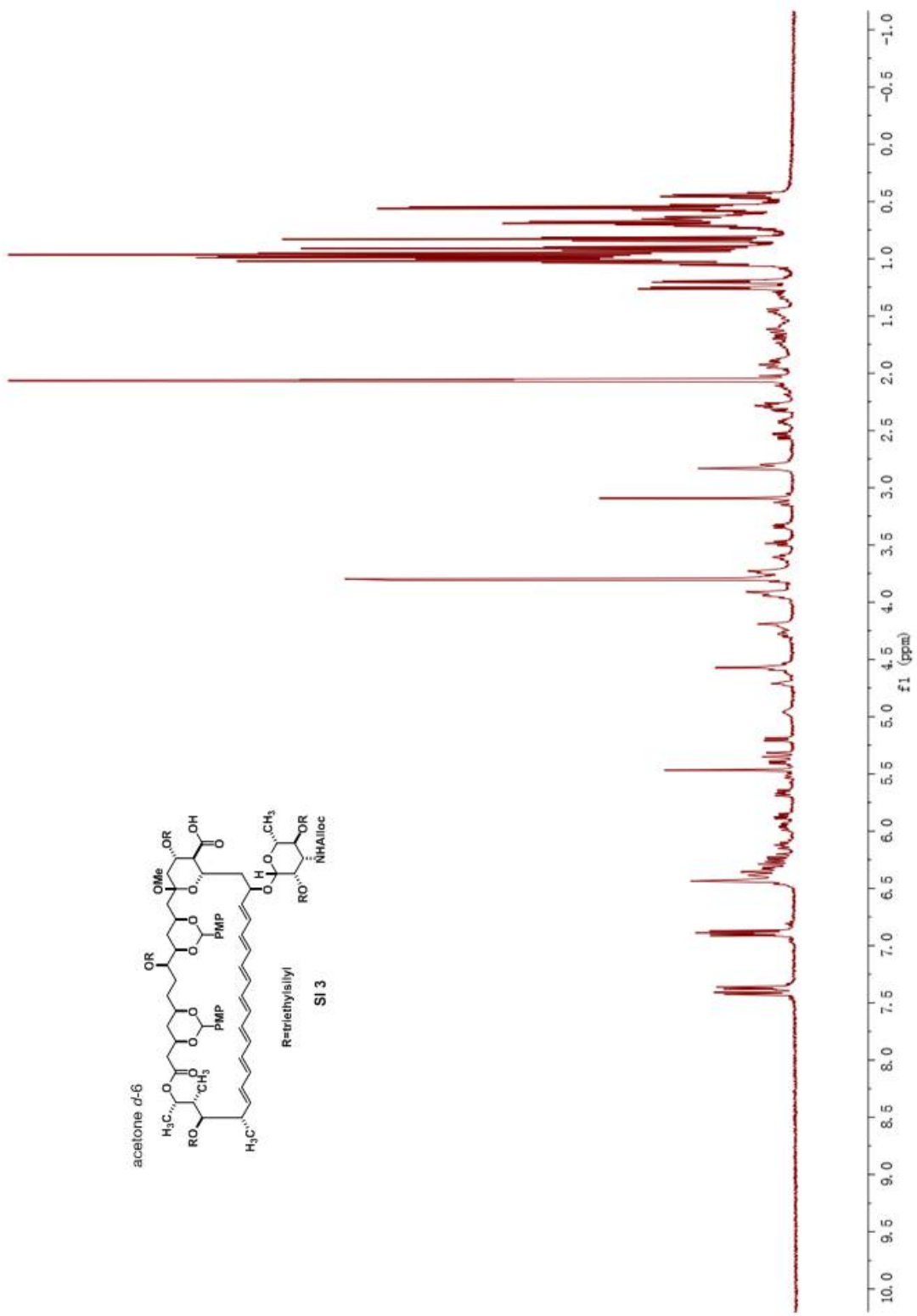
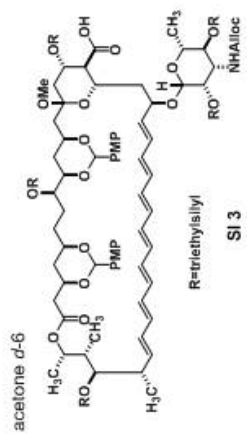
81	AmBH24-H7b	2.9E+07		
82	AmBH25-H7b	1.8E+07	C3AmBH7b-H25	3.0E+07
83	AmBH26-H7b	2.4E+07	C3AmBH7b-H26	7.5E+07
84	AmBH8-H9	1.2E+08	C3AmBH8-H9	2.0E+08
85	AmBH8-H10a	6.3E+07	C3AmBH8-H10a	1.1E+08
86	AmBH8-H10b	9.0E+07	C3AmBH8-H10b	2.5E+08
87	AmBH8-H11	1.4E+07	C3AmBH8-H11	2.4E+07
88	AmBH8-H12a	5.1E+06	C3AmBH8-H12a	2.3E+07
89	AmBH8-H12b	9.6E+06	C3AmBH8-H12b	1.2E+07
90	AmBH9-H10a	2.2E+07	C3AmBH9-H10a	6.4E+07
91	AmBH9-H10b	4.0E+07	C3AmBH9-H10b	1.4E+08
92	AmBH9-H11	1.6E+08	C3AmBH9-H11	2.5E+08
93	AmBH9-H12a	7.8E+06		
94	AmBH9-H12b	1.6E+07	C3AmBH9-H12b	3.0E+07
95	AmBH9-H20	8.3E+06	C3AmBH20-H9	2.3E+07
96			C3AmBH9-H21	5.7E+06
97	AmBH9-H22	6.2E+07	C3AmBH9-H22	8.5E+07
98	AmBH9-H23	6.3E+06		
99	AmBH9-H24	4.6E+07	C3AmBH9-H24	9.0E+07
100	AmBH9-H25	1.2E+07		
101	AmBH9-H26	8.8E+06	C3AmBH9-H26	1.6E+07
102	AmBH10a-H10b	2.3E+08	C3AmBH10a-H10b	7.5E+08
103	AmBH10a-H11	5.9E+07	C3AmBH10a-H11	8.6E+07
104	AmBH10a-H12a	1.9E+08	C3AmBH10a-H12a	2.7E+08
105	AmBH10a-H12b	7.2E+07	C3AmBH10a-H12b	1.3E+08
106	AmBH10a-H14a	1.1E+07	C3AmBH10a-H14a	3.2E+07
107			C3AmBH10a-H14b	1.3E+07
108	AmBH10b-H11	7.8E+07	C3AmBH10b-H11	1.7E+08
109	AmBH10b-H12a	5.4E+07		
110	AmBH10b-H12b	1.0E+08	C3AmBH10b-H12b	2.4E+08
111			C3AmBH22-H10b	6.5E+06
112	AmBH10b-H14b	5.2E+06		
113			C3AmBH24-H10b	5.0E+06
114	AmBH11-H12a	4.4E+07	C3AmBH11-H12a	7.3E+07
115	AmBH11-H12b	1.2E+08	C3AmBH11-H12b	1.5E+08
116	AmBH11-H14a	1.4E+07	C3AmBH11-H14a	2.9E+07
117	AmBH11-H14b	8.2E+06	C3AmBH11-H14b	1.6E+07
118			C3AmBH11-H16	6.1E+06
119	AmBH11-H17	2.5E+07	C3AmBH11-H17	2.2E+07
120			C3AmBH11-H18a	6.2E+06
121	AmBH11-H18b	1.8E+07	C3AmBH11-H18b	1.4E+07
122	AmBH20-H11	7.3E+07	C3AmBH11-H20	1.2E+08
123	AmBH21-H11	1.1E+07	C3AmBH11-H21	1.5E+07
124	AmBH22-H11	6.0E+07	C3AmBH11-H22	9.7E+07
125			C3AmBH11-H24	2.5E+07
126			C3AmBH12a-H10b	1.6E+08
127	AmBH12a-H12b	5.3E+08	C3AmBH12a-H12b	7.5E+08
128	AmBH12a-H14a	9.2E+07	C3AmBH12a-H14a	1.8E+08
129	AmBH12a-H14b	8.0E+07	C3AmBH12a-H14b	2.1E+08
130	AmBH12a-H15	7.1E+06	C3AmBH12a-H15	2.8E+07
131	AmBH12a-H16	4.6E+06	C3AmBH12a-H16	6.3E+06
132	AmBH12a-H17	5.8E+06	C3AmBH12a-H17	9.0E+06
133			C3AmBH12a-H9	3.6E+07
134	AmBH12b-H14a	2.8E+08	C3AmBH12b-H14a	3.0E+08
135	AmBH12b-H14b	6.7E+07	C3AmBH12b-H14b	1.4E+08
136	AmBH12b-H15	1.1E+07	C3AmBH12b-H15	2.2E+07
137			C3AmBH12b-H16	2.1E+07
138	AmBH12b-H17	4.5E+06	C3AmBH12b-H17	7.9E+06
139			C3AmBH12b-H20	1.3E+07
140	AmBH14a-H14b	4.5E+08	C3AmBH14a-H14b	8.4E+08
141	AmBH14a-H15	3.9E+07	C3AmBH14a-H15	9.6E+07
142	AmBH14a-H16	9.1E+07	C3AmBH14a-H16	1.4E+08
143	AmBH14a-H17	7.1E+06	C3AmBH14a-H17	1.5E+07
144	AmBH14b-H15	1.6E+08	C3AmBH14b-H15	2.4E+08
145			C3AmBH14b-H16	4.8E+07
146	AmBH14b-H17	9.2E+06	C3AmBH14b-H17	1.9E+07
147	AmBH15-H16	4.4E+07		
148	AmBH15-H17	1.5E+08		
149	AmBH16-H17	2.0E+07	C3AmBH16-H17	4.9E+07
150	AmBH16-H18a	2.8E+07	C3AmBH16-H18a	8.3E+07
151	AmBH16-H18b	5.5E+07	C3AmBH16-H18b	1.0E+08
152	AmBH16-H101	4.3E+06	C3AmBH16-H101	8.3E+06
153			C3AmBH16-H102	3.3E+06
154	AmBH17-H18a	3.5E+07	C3AmBH17-H18a	8.8E+07
155	AmBH17-H18b	3.1E+07	C3AmBH17-H18b	6.8E+07
156	AmBH17-H20	7.2E+07	C3AmBH17-H20	1.1E+08
157	AmBH17-H21	9.7E+06	C3AmBH17-H21	1.0E+07
158	AmBH17-H22	7.5E+06	C3AmBH17-H22	1.2E+07
159	AmBH101-H17	3.8E+07	C3AmBH17-H101	4.8E+07
160	AmBH17-H102	2.0E+07	C3AmBH102-H17	3.9E+07

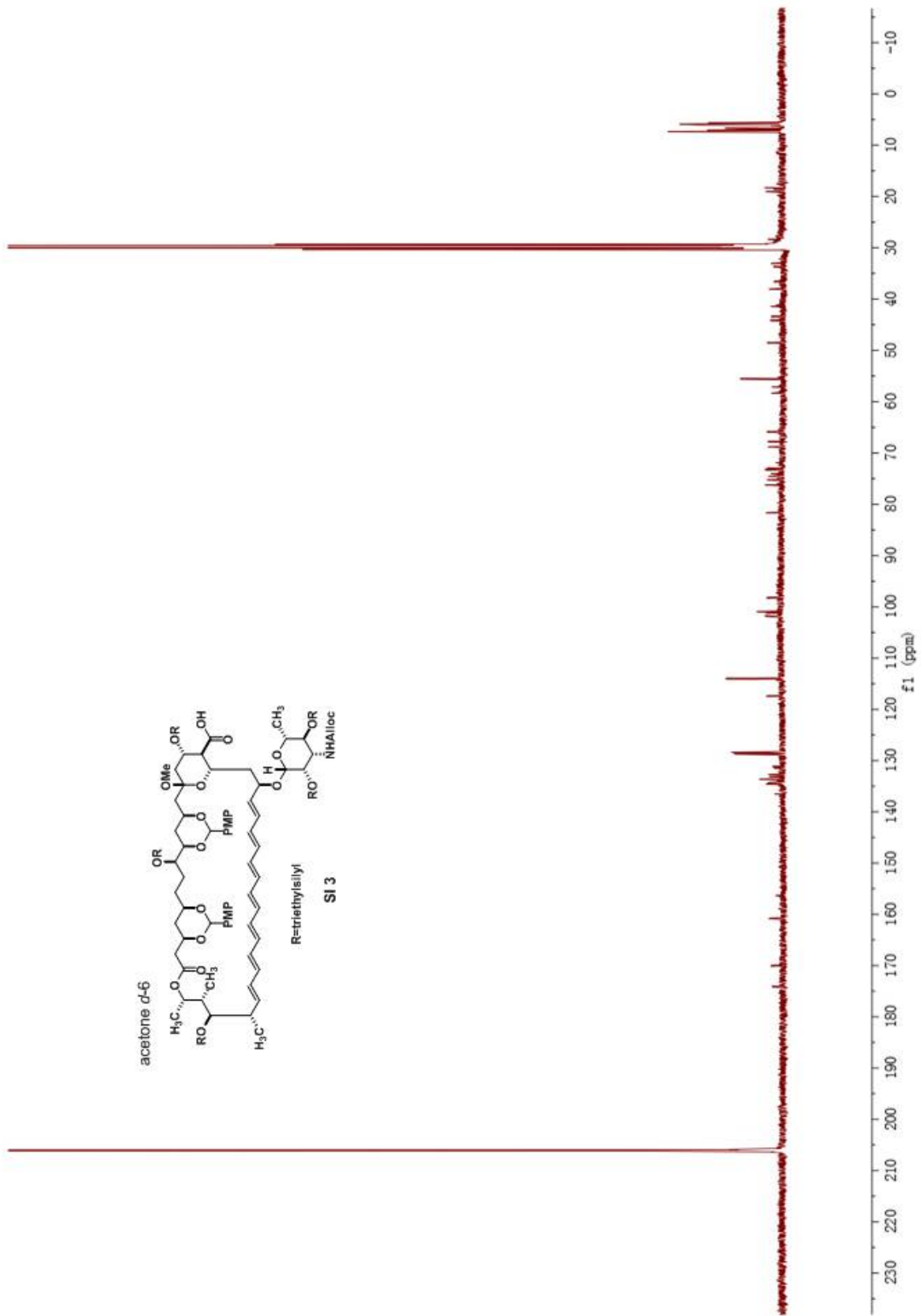
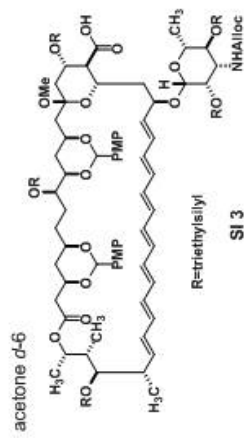
161	AmBH18a-H18b	4.6E+08	C3AmBH18a-H18b	1.3E+09
162	AmBH18a-H19	9.9E+07	C3AmBH18a-H19	1.9E+08
163	AmBH18b-H19	7.6E+07	C3AmBH18b-H19	1.9E+08
164	AmBH18a-H20	1.3E+07	C3AmBH18a-H20	1.9E+07
165	AmBH18a-H21	1.2E+07	C3AmBH18a-H21	2.1E+07
166	AmBH18b-H20	1.9E+07	C3AmBH18b-H20	2.9E+07
167	AmBH18b-H21	2.1E+07	C3AmBH18b-H21	3.3E+07
168	AmBH18a-H101	8.2E+07	C3AmBH18a-H101	1.9E+08
169	AmBH18a-H102	8.4E+06	C3AmBH102-H18a	2.3E+07
170	AmBH18b-H101	3.8E+07	C3AmBH18b-H101	8.5E+07
171	AmBH18b-H102	9.9E+06	C3AmBH18b-H102	1.1E+07
172	AmBH19-H20	6.3E+07	C3AmBH19-H20	7.2E+07
173	AmBH19-H21	2.2E+08	C3AmBH19-H21	3.3E+08
174	AmBH19-H22	8.7E+06	C3AmBH19-H22	1.4E+07
175			C3AmBH19-H23	1.9E+07
176	AmBH19-H101	1.2E+08	C3AmBH19-H101	2.0E+08
177	AmBH19-H102	2.0E+07	C3AmBH19-H102	1.6E+07
178			C3AmBH19-H106	1.2E+07
179	AmBH20-H101	5.6E+06	C3AmBH20-H101	1.2E+07
180	AmBH20-H102	2.9E+06	C3AmBH20-H102	5.1E+06
181			C3AmBH21-H101	1.6E+07
182			C3AmBH21-H22	6.7E+07
183			C3AmBH24-H26	3.1E+08
184			C3AmBH25-H26	4.5E+08
185			C3AmBH25-H6b	1.0E+07
186			C3AmBH26-H6b	1.0E+07
187			C3AmBH31-H32	1.3E+09
188	AmBH31-H33	1.7E+08	C3AmBH31-H33	2.5E+08
189	AmBH31-H34	2.8E+07	C3AmBH31-H34	4.4E+07
190	AmBH31-H35	7.3E+06	C3AmBH31-H35	9.7E+06
191	AmBH31-H36	1.3E+07	C3AmBH31-H36	1.8E+07
192	AmBH31-H40	1.0E+07	C3AmBH31-H40	2.0E+07
193	AmBH32-H33	7.7E+07	C3AmBH32-H33	1.1E+08
194	AmBH32-H34	2.7E+08	C3AmBH32-H34	3.8E+08
195	AmBH32-H35	1.1E+07	C3AmBH32-H35	1.5E+07
196	AmBH32-H36	3.3E+07	C3AmBH32-H36	4.0E+07
197			C3AmBH32-H37	1.7E+08
198	AmBH32-H38	1.3E+07	C3AmBH32-H38	2.0E+07
199	AmBH32-H39	6.2E+06		
200	AmBH32-H40	3.7E+07	C3AmBH32-H40	4.8E+07
201	AmBH33-H34	3.2E+07	C3AmBH33-H34	4.6E+07
202	AmBH33-H35	9.0E+07	C3AmBH33-H35	1.3E+08
203	AmBH33-H36	5.6E+07	C3AmBH33-H36	8.3E+07
204	AmBH37-H33	2.5E+07		
205	AmBH33-H39	1.1E+07	C3AmBH33-H39	1.7E+07
206	AmBH33-H40	1.1E+08	C3AmBH33-H40	1.6E+08
207	AmBH34-H35	3.3E+07	C3AmBH34-H35	4.7E+07
208	AmBH34-H36	4.4E+07	C3AmBH34-H36	4.3E+07
209	AmBH34-H37	2.0E+08	C3AmBH34-H37	3.1E+08
210	AmBH34-H38	2.3E+07	C3AmBH34-H38	3.1E+07
211			C3AmBH34-H39	1.6E+07
212	AmBH34-H40	8.7E+07	C3AmBH34-H40	1.7E+08
213	AmBH35-H36	1.3E+08	C3AmBH35-H36	2.7E+08
214	AmBH35-H37	1.4E+07	C3AmBH35-H37	2.0E+07
215	AmBH35-H38	8.0E+06	C3AmBH35-H38	1.1E+07
216	AmBH35-H39	5.7E+07	C3AmBH35-H39	1.2E+08
217	AmBH35-H40	5.5E+07	C3AmBH35-H40	1.2E+08
218	AmBH36-H37	6.7E+07	C3AmBH36-H37	1.1E+08
219	AmBH36-H38	2.1E+07	C3AmBH36-H38	3.9E+07
220	AmBH36-H39	1.4E+08	C3AmBH36-H39	2.0E+08
221	AmBH36-H40	1.7E+07	C3AmBH36-H40	1.9E+07
222			C3AmBH37-H31	1.8E+07
223	AmBH37-H38	8.1E+07	C3AmBH37-H38	1.8E+08
224	AmBH37-H39	1.7E+07	C3AmBH37-H39	2.9E+07
225	AmBH37-H40	1.3E+07	C3AmBH37-H40	1.6E+07
226			C3AmBH38-H31	5.0E+06
227	AmBH38-H39	7.8E+07	C3AmBH38-H39	1.2E+08
228			C3AmBH39-H31	5.7E+06
229			C3AmBH39-H32	1.2E+07
230	AmBH101-H102	5.0E+07	C3AmBH101-H102	1.3E+08
231	AmBH101-H104	9.8E+06	C3AmBH101-H104	1.8E+07
232	AmBH101-H106	6.4E+06	C3AmBH101-H106	1.5E+07
233	AmBH102-H104	8.3E+06	C3AmBH102-H104	1.4E+07
234	AmBH102-H106	3.4E+06	C3AmBH102-H106	4.6E+06
235	AmBH104-H106	5.2E+07	C3AmBH104-H106	8.5E+07

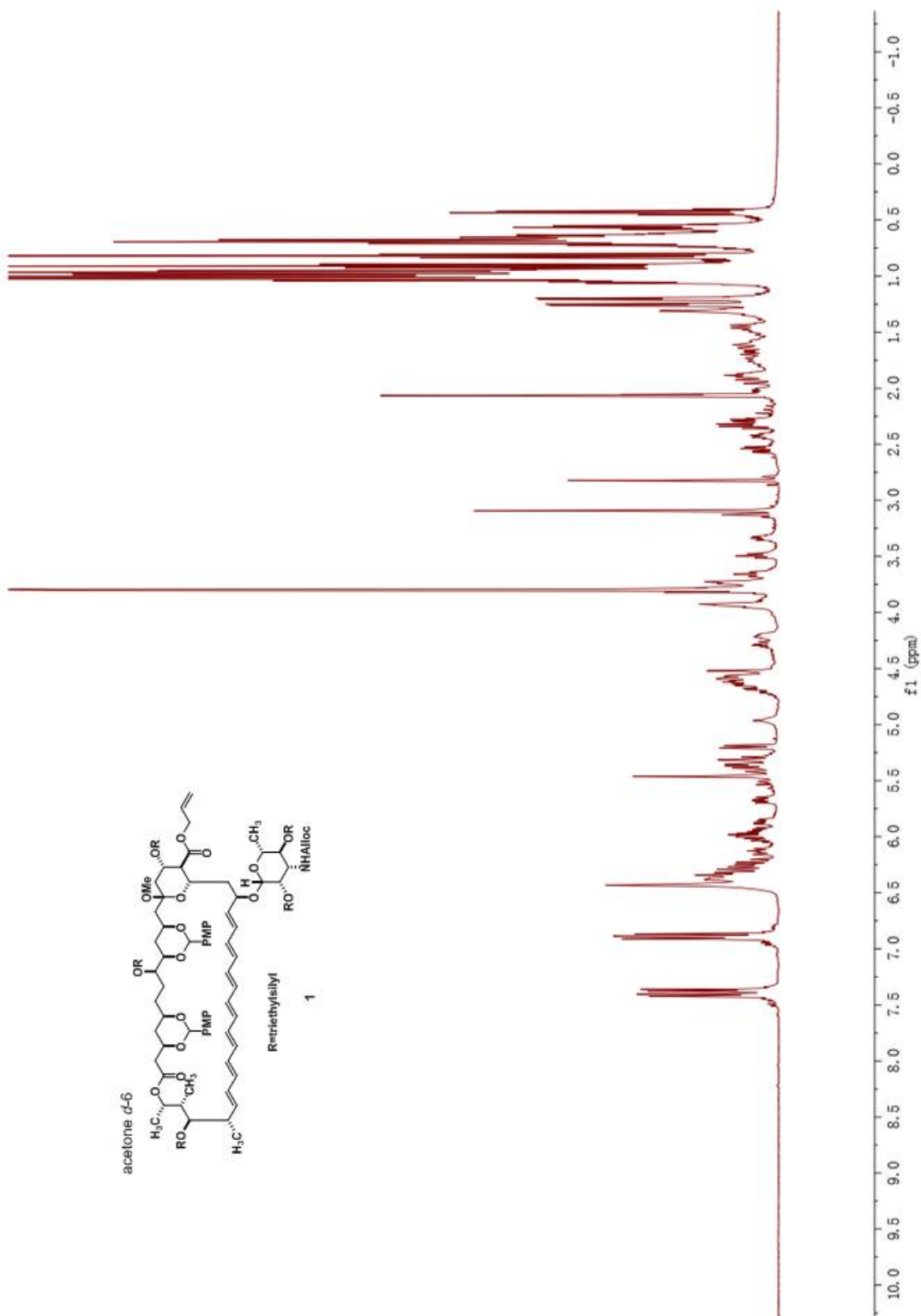
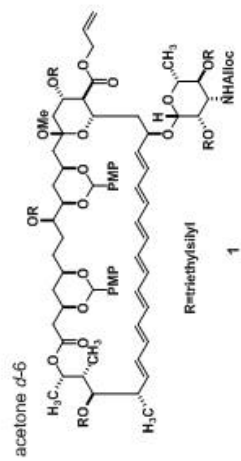
III. NMR Spectra of New Compounds

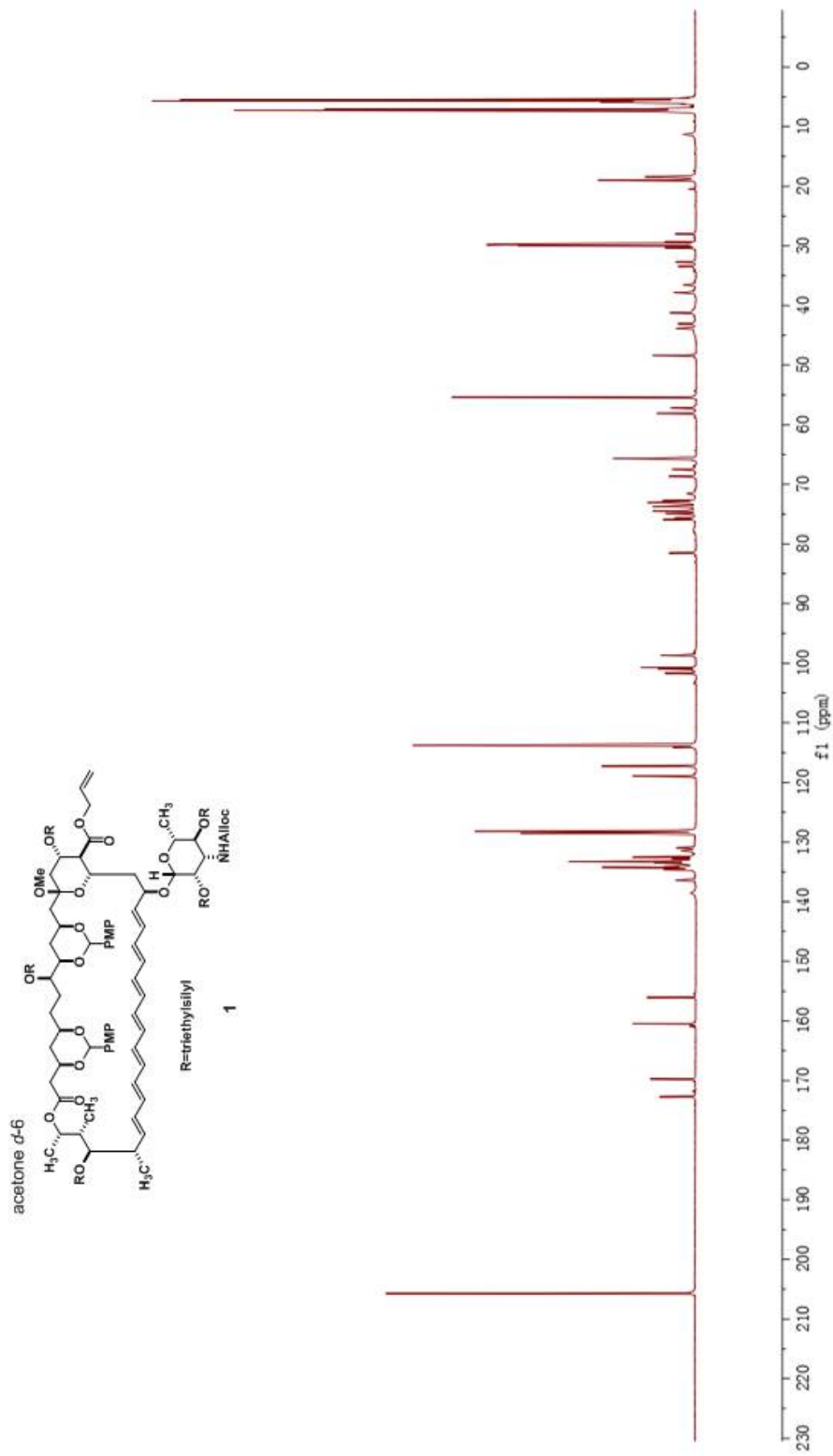


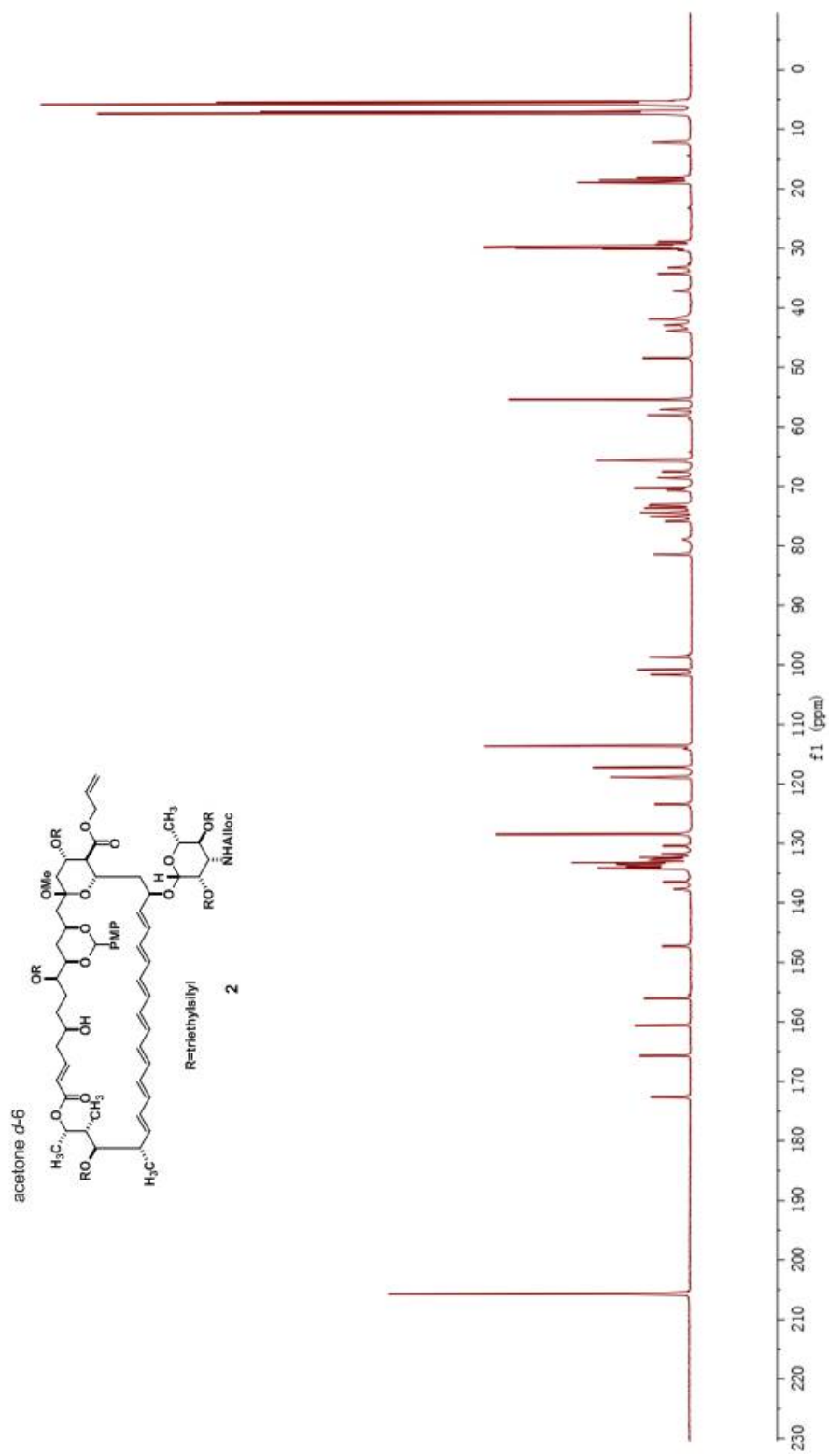


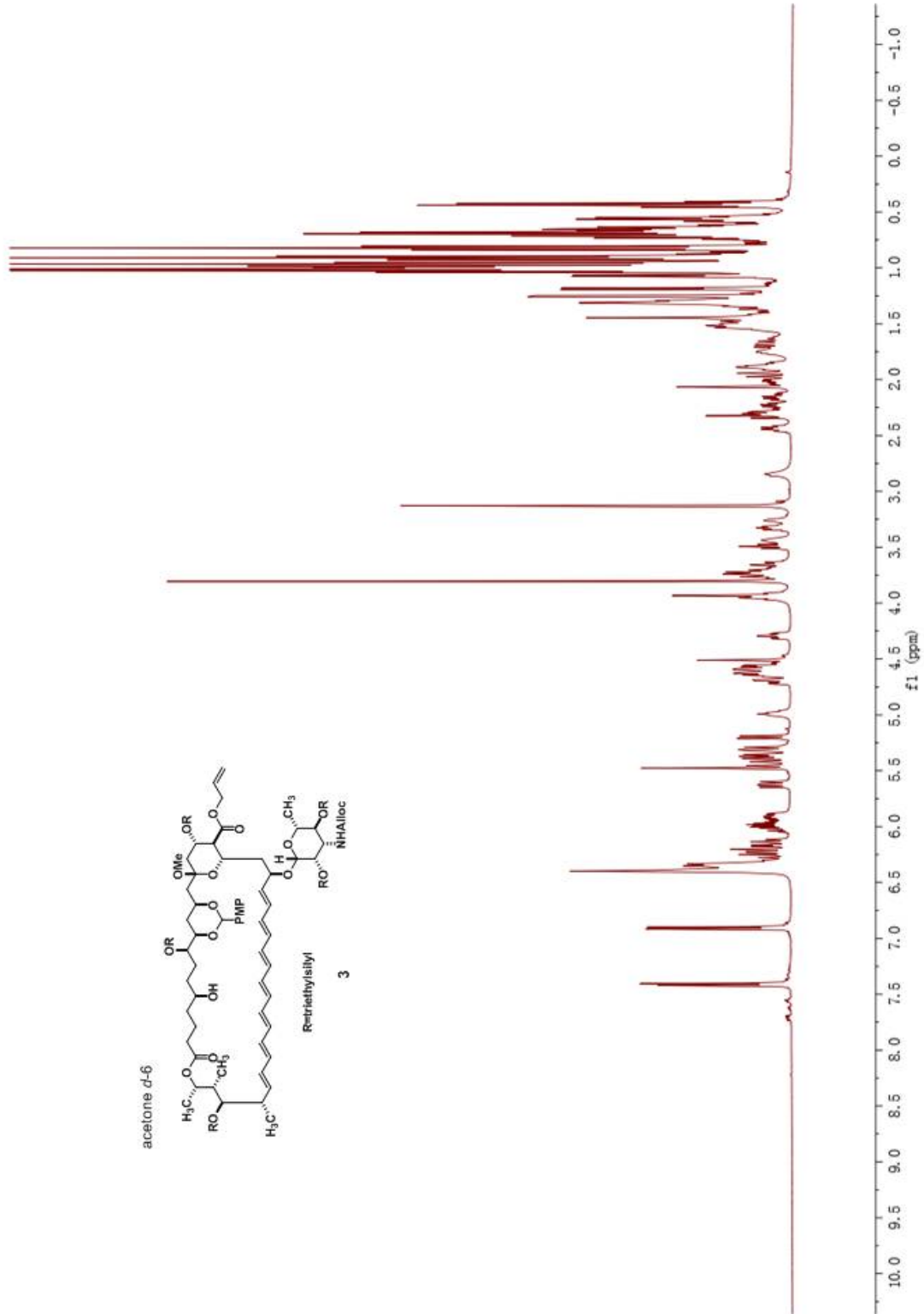
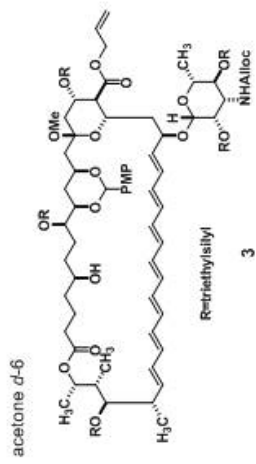


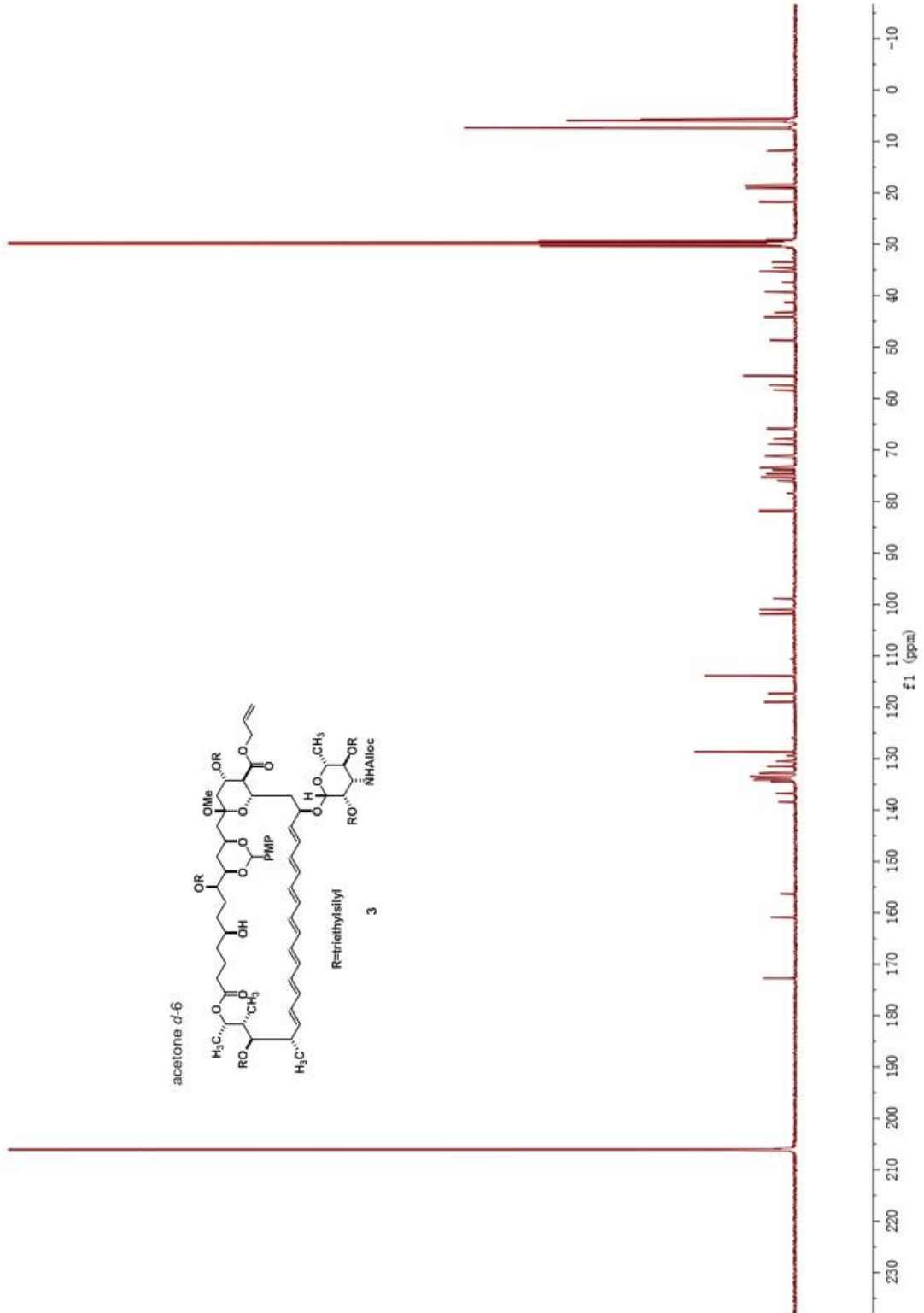
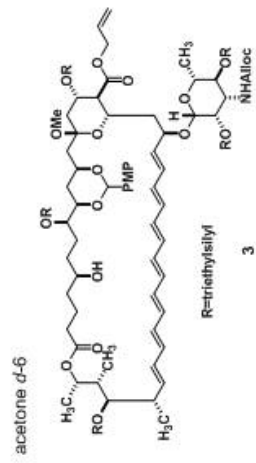




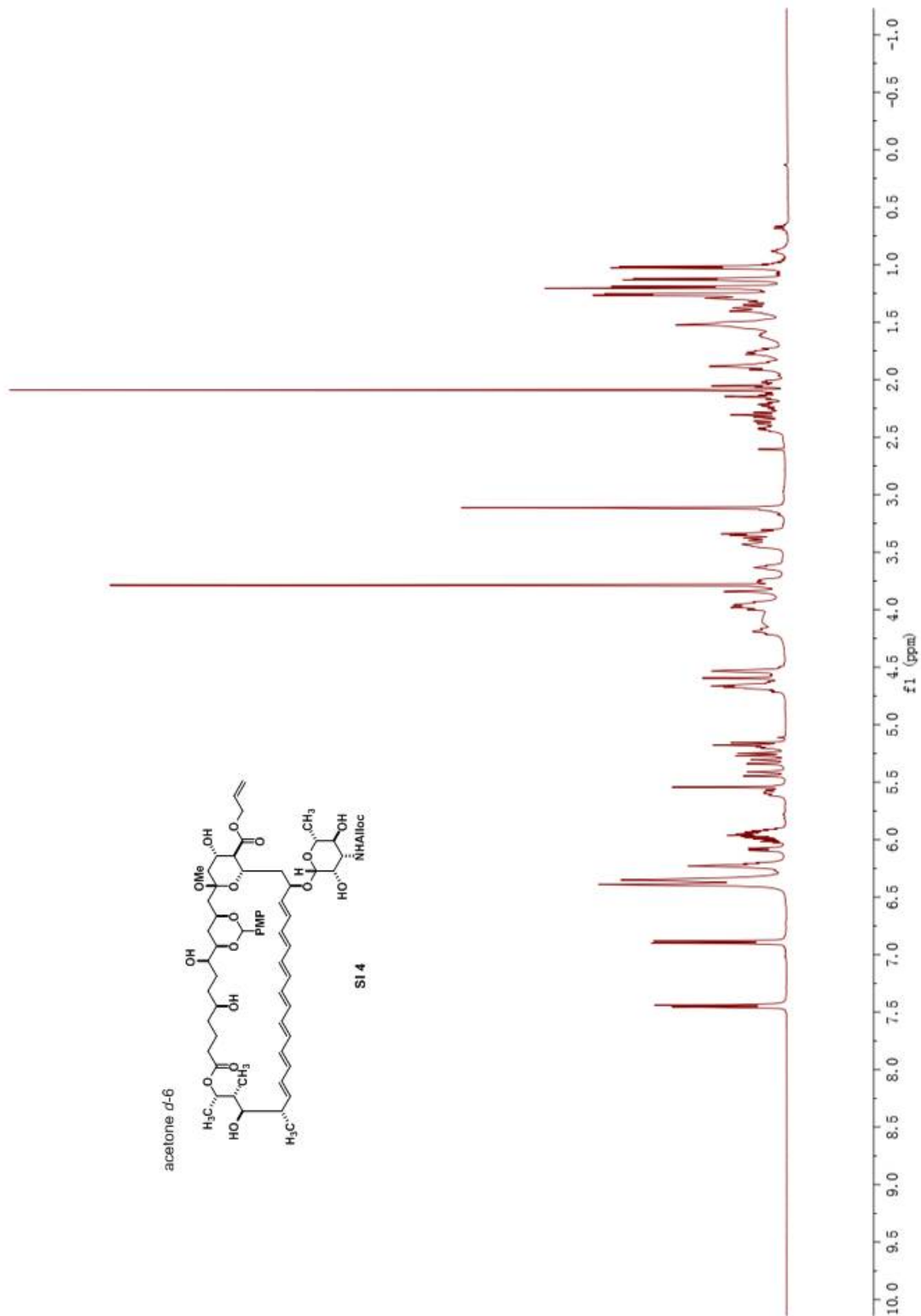
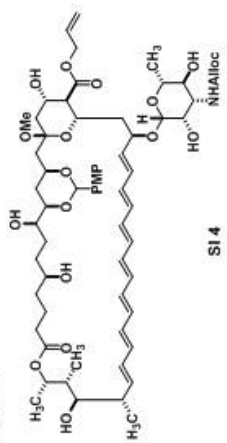


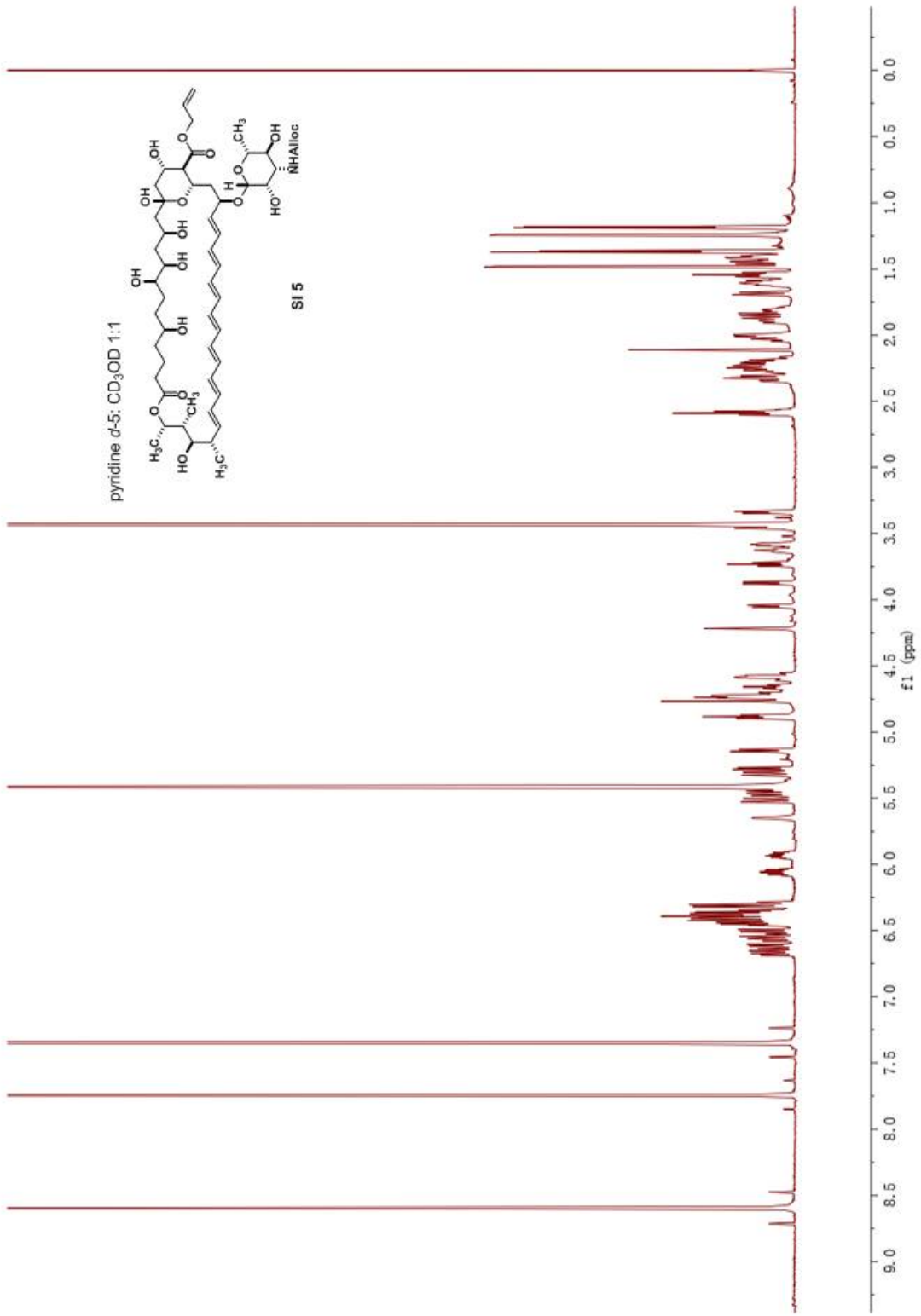


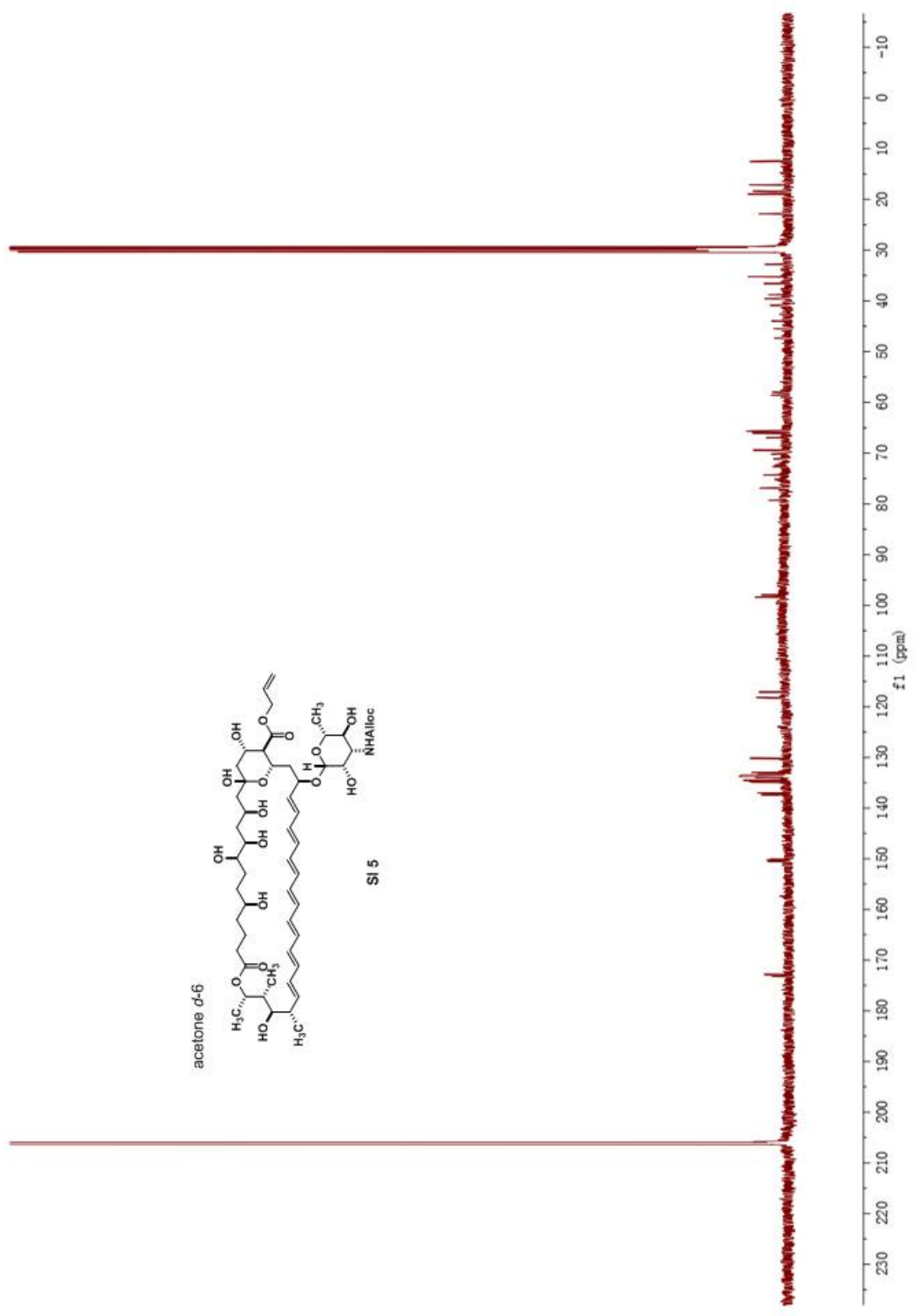
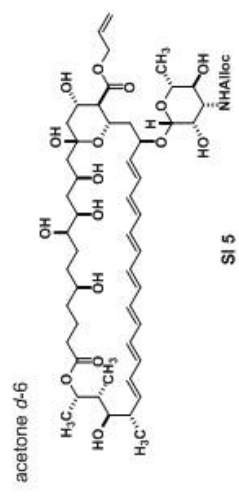




acetone *d*-6







References

1. Pangborn, A. B.; Giardello, M. A.; Grubbs, R. H.; Rosen, R. K.; Timmers, F. J. *Organometallics* **1996**, *15*, 1518.
2. Still, W. C.; Kahn, M.; Mitra, A. *J. Org. Chem.* **1978**, *43*, 2923.
3. (a) L. N. Ermishkin; Kasumov, K. M.; Potzeluyev, V. M. *Nature* **1976**, *262*, 698. (b) Ermishkin, L. N.; Kasumov, K. M.; Potseluyev, V. M. *Biochim. Biophys. Acta, Biomembr.* **1977**, *470*, 357. (c) Borisova, M. P.; Ermishkin, L. N.; Silberstein, A. Y. *Biochim. Biophys. Acta, Biomembr.* **1979**, *553*, 450. (d) Kasumov, K. M.; Borisova, M. P.; Ermishkin, L. N.; Potseluyev, V. M.; Silberstein, A. Y.; Vainshtein, V. A. *Biochim. Biophys. Acta* **1979**, *551*, 229. (e) Borisova, M. P.; Brutyan, R. A.; Ermishkin, L. N. *J. Membr. Biol.* **1986**, *90*, 13. (f) Mickus, D. E.; Levitt, D. G.; Rychnovsky, S. D. *J. Am. Chem. Soc.* **1992**, *114*, 359. (g) Brutyan, R. A.; McPhie, P. *J. Gen. Physiol.* **1996**, *107*, 69. (h) Ibragimova, V.; Alieva, I.; Kasumov, K.; Khutorsky, V. *Biochim. Biophys. Acta, Biomembr.* **2006**, *1758*, 29.
4. Chen, P.S.; Toribara, T.Y.; Warner, H. *Anal. Chem.* **1956**, *28*, 1756.
5. Delaglio, F.; Grzesiek, S.; Vuister, G. W.; Zhu, G.; Pfeifer, J.; Bax, A. *J. Biomol. NMR.* **1995**, *6*, 277.
6. Goddard, T. D.; Kneller, D. G. SPARKY 3, University of California, San Francisco <http://www.cgl.ucsf.edu/home/sparky/>.
7. Delaglio, F.; Wu, Z.; Bax, A. *J. Magn. Reson.* **2001**, *149*, 276.
8. Palacios, D. S.; Anderson, T. M.; Burke, M. D. *J. Am. Chem. Soc.* **2007**, *129*, 13804.
9. Navarro-Vazquez, A.; Cobas, J. C.; Sardina, F. J. *J. Chem. Info. Comput. Sci.* **2004**, *44*, 1680.
10. Labute, P. *J. Chem. Info. Model.* **2010**, *50*, 792.
11. Molecular Operating Environment (MOE), 2013.08; Chemical Computing Group Inc., 1010 Sherbooke St. West, Suite #910, Montreal, QC, Canada, H3A 2R7, 2015.
12. Jarzemska, K. N.; Kaminski, D.; Hoser, A. A.; Malinska, M.; Senczyna, B.; Wozniak, K.; Gagos, M. *Cryst. Growth Des.* **2012**, *12*, 2336.
13. Humphrey, W., Dalke, A. and Schulten, K., "VMD - Visual Molecular Dynamics", *J. Molec. Graphics*, **1996**, *14*, 33.